Department of Physical Geography
and Quaternary Geology

Stockholm
University

The Impacts of Climate Change on River Flow and Riparian Vegetation in the Amu Darya River Delta, Central Asia

Ye Su

Master's thesis
Physical Geography and Quaternary Geology, 45 HECs

NKA 54
2012

Department of Physical Geography and Quaternary Geology

Stockholm University

Preface

This Master's thesis is Ye Su's degree project in Physical Geography and Quaternary Geology, at the Department of Physical Geography and Quaternary Geology, Stockholm University. The Master's thesis comprises 45 HECs (one and a half term of full-time studies).

Supervisor has been Jerker Jarsjö at the Department of Physical Geography and Quaternary Geology, Stockholm University. Examiner has been Steve Lyon, at the Department of Physical Geography and Quaternary Geology, Stockholm University.

The author is responsible for the contents of this thesis.

Stockholm, 21 February 2012

Lars-Ove Westerberg
Director of studies

Abstract

The increasing global air temperature will trigger changes in the global mean water vapor, precipitation patterns and evapotranspiration, which further leads to changes, for instance, in stream flow, groundwater flow and soil moisture. Projections of future changes in the hydrological regime of the Aral Sea Drainage Basin (ASDB) in Central Asia are however highly uncertain, due to complexities of natural and engineered water systems of the basin. The Amu Darya River Delta (ADRD) is vital to the water budget of the Large Aral Sea, the livelihood in Uzbekistan and Turkmenistan, as well as the surrounding riparian ecosystem. This study attempts to investigate responses of river flow in the Aral Sea Drainage Basin and key riparian vegetation species (of the so-called Tugai community) in the Amu Darya River Delta to projected future climate change. Results from hydrological model and outputs from multi-GCM predictions provide a basis for conducting more robust quantitative analysis of possible future hydro-climatic changes in the Amu Darya River Basin. A qualitative synthesis of the suitability of Tugai is furthermore performed in order to increase the knowledge of the riparian vegetation status under the changing hydro-climatic conditions. The results show that the averaged temperature in the ASDB is likely to continuously increase and yield a total increase of about 2 °C ~ 5°C by 2100. The change trend of the annual regional precipitation of 2100 is relatively unclear, with estimates ranging from 50 mm lower than today to 75 mm higher than today. Modeled ensemble means (EM) river flow, obtained from hydrological modeling of climate output from multi-GCM projections, converge on showing future decreases in river runoff (R). Projected absolute R may decrease to zero around 2100, implying no surface flow and a dry out near the river outlet. The relationship of water flux between upstream and downstream will be changed dramatically due to climate change. More specifically, R of the upstream region will decrease, and it is likely to become insufficient for feeding downstream river reaches as it used to. The decreased river flow in the delta may accelerate the desertification and salinization processes. Consequently, species transitions may occur, along with degradations of the existing Tugai communities. The uncertainties of hydro-climatic change projections to some extent hinder the understanding of the dynamic hydrological-climatic-ecological system. However, the detailed responses of the delta to climate change based on multiple qualitative and quantitative analyses provide an important basis for the formulation of more robust forecasts on the future ecological development in the ADRD, and further for recommendations of measures to mitigate the ecosystem's deterioration under a changing climate.

Key words

Climate change, GCM, Aral Sea Drainage Basin, Amu Darya River Delta, river flow, Tugai

Contents

PREFACE ---------- **III**

ABSTRACT ---------- **V**

KEY WORDS ---------- **V**

ABBREVIATIONS ---------- **VIII**

LIST OF FIGURES AND TABLES ---------- **IX**

1. INTRODUCTION ---------- **1**

2. STUDY SITE ---------- **5**

2.1 The Aral Sea Drainage Basin ---------- 5

2.2 The Amu Darya River Basin ---------- 7

2.3 The Amu Darya River Delta ---------- 8

2.4 Tugai community in the Amu Darya River Delta ---------- 10

3. MATERIALS AND METHODS ---------- **13**

3.1 The multi-GCM projections of future hydro-climatic changes ---------- 14

3.2 Hydrological modelling ---------- 16

3.3 Hydrological Response Map ---------- 19

3.4 Riparian vegetation qualitative analysis approach ---------- 20

4. RESULTS ---------- **21**

4.1 Current hydro-climatic conditions ---------- 21

4.2 The changing regional climate ---------- 22

4.3 Results of different hydrological conditions under different climatic scenarios ---------- 25

4.4 Prediction of Tugai community's development based on their suitability ---------- 31

5. DISCUSSION ---------- **34**

5.1 Hydro-climate dynamics in the Amu Darya River Basin ---------- 34

5.2 Uncertainty of GCMs driven projections on hydro-climatic condition ---------- 35

5.3 Ecosystem management in the Amu Darya River Delta ---------- 37

6. CONCLUSION SUMMARY ---------- **39**

ACKNOWLEDGEMENTS ---------- **41**

REFERENCES ---------- **42**

APPENDIX ---------- **47**

Abbreviations

Amu Darya River Basin	ADRB
Amu Darya River Delta	ADRD
Aral Sea Drainage Basin	ASDB
Averaged Ensemble Mean	EM
Climate Research Unit	CRU
Coefficient of Variation	CV
Evapotranspiration	ET
Geographic Information System	GIS
Global Climate Model/General Circulation Model	GCM
Global Map of Irrigated Areas	GMIA
Global Runoff Data Centre	GRDC
Ground Water	GW
Ground Water Table	GWT
Hectares (100 ha =1 km^2)	ha
International Panel on Climate Change	IPCC
Precipitation	P
Potential Evapotranspiration	ET_p
Regional Climate Model	RCM
River Runoff	R
Shuttle Rader Topography Mission	SRTM
Standard Deviation	SD
Temperature	T
Tyuyamuyun Hydroengineering Complex	THC

List of figures and tables

Fig. 1 Map of the Aral Sea Drainage Basin 5
Fig. 2 Map of Amu Darya River Basin (ADRB) and its delta 7
Fig. 3 The distribution of Tugai forests in the Amu Darya River Delta and its landscapes . 9
Fig. 4 The Phytomorph of different Tugai species in each community formation and their status 11
Fig. 5 Conceptual framework of this study 13
Fig. 6 Distributed maps of present hydro-climate conditions in the ASDB 21
Fig. 7 The long term and short term predictions of climate change in the Central Asia and the ASDB 23
Fig. 8 The modeled changes of ET under two wet and two dry scenarios 25
Fig. 9 The modeled changes of PS under two wet and two dry scenarios 27
Fig. 10 Comparison of the changed ET and PS under two wet and two dry scenarios 28
Fig. 11 The trend of estimated Hydrological Response Map for △R in the ADRD 29
Fig. 12 Changes of the absolute R for three studied locations 30

Table 1 The matrix of $\triangle T_i$ and $\triangle P_j$ for producing a hydrological response map. 19
Table 2 The detailed values of each studied climate change scenarios 24
Table 3 Suitability factors of Tugai 32

Appendix 1 The comparison of modeled absolute values of river runoff in each study sites -- 47

1. Introduction

As the earth has experienced a global averaged temperature increase of approximately 0.74 [0.56 ~ 0.92] °C over the last 100 years, a number of effects accompanying this warming have been observed and studied from manifold scientific standpoints (IPCC, 2003; IPCC, 2007a). A recently published set of greenhouse gas (GHG) emission scenarios in the 4th International Panel on Climate Change (IPCC) report (IPCC, 2007a), have projected that an overall trend of the annual mean temperature is likely to continuously increase, yielding a total increase between 1.1°C and 6.4°C by 2100 in comparison with the period with 1980 ~ 1990. However, climate change predictions still give rise to controversies in the scientific media in the light of uncertainties towards the extent of variations. This is due to the uncertainties on climate sensitivity as well as on how human activities will be developed under different conditions to respond the changing climate (Nakagawa et al., 2003, Nijssen et al., 2001). In recent years, different Global Climate Models (or General Circulation Models, GCMs) have been developed and operated to generate alternative scenarios of global climate change (e.g. more than 34 GCMs are developed by 14 different climatology research centers) (IPCC, 2003; 2007a). However, the variable regional geography, topography and geology across the globe result in an uneven distribution of climatic variables in time and space (IPCC, 2007b). Therefore, the variability of climate at regional scales, either for the past, the present or for the future, is more critical and hard to examine than the averaged global climate. Furthermore, the plausible climate change projections and the analyses of its effects in certain regions are considered during the decision making process, and provide an important basis for future regional development planning (Milly et al., 2005).

A key question in the light of climate change predictions is how the hydrological cycle will respond to changes in climatic driving variables such as temperature and precipitation. A series of researches confidently pointed out that the increasing global air temperature will trigger changes in, for instance, the global mean water vapor, precipitation patterns and evapotranspiration (IPCC, 2007a; Arora and Boer, 2001; Savitsky et al., 2007; Arnell, 2003). Consequently, the core climatological driving variables being the main factors influence each interacted role within the hydrological cycle's performances in terms of stream flow, groundwater flow and soil moisture. Furthermore, the climate-induced hydrological simulation offers an effective approach to evaluate the water balance in hydrological system as well as the availability and the vulnerability of water resources in river basins under a changing climate (Arora and Boer, 2001).

Stakhiv et al. (1992) and Van (1999) concluded that river basins in arid and semi-arid regions would be strongly affected by changing climate on the hydrological regimes even under relatively small climatic variations. Additionally, Arora and Boer (2001) simulated the discharge for twenty-three major catchments in the world and concluded that a general reduction on annual mean discharge over some dry regions at mid-latitudes and dry tropics may occur as a result of projected climate changes. On the whole, IPCC (2007b) revealed that river runoff for Central Asia is likely to decrease with 10 ~ 30% by 2050, and stated that the frequency and severity of extreme events will rise. Multiple research results from global-scale predictions converge on showing that Central Asia is one of the vulnerable regions influenced by global warming (Lioubimtseva and Henebry, 2009). Natural landscape transitions or anthropogenic changes in land and water utilization of Central Asia over the last 5 decades (for instance, the expansion of large-scale irrigated fields) has exacerbated the vulnerability of such arid regions to react even to relatively minor climate variations, particularly in the western parts of Turkmenistan, Uzbekistan, and Kazakhstan (Lioubimtseva and Henebry, 2009; Jarsjö et al., 2011, Kulmatov, 2009). Hence, projections of probable changes in the hydrological regime in Central Asia will remain highly uncertain, due to its arid nature and because of a lack of historical observation data (IPCC, 2007a). Moreover, Central Asia's severe environmental crises, e.g. the shrinkage of the Aral Sea, stream flow decrease, desertification, contamination, salinization and ecosystem degradation, in the past century are gradually damaging the well-balanced responses and natural resilience. Consequently, the hydrological response in Central Asia's basins to climate change will be relatively severe, fast and sensitive, as a result, which requires more research activities to study the system holistically.

In addition, climatic change can shift riparian vegetation patterns as a result of water system changes such as changed groundwater table, water quality, frequency or quantity of flooding, and soil moisture (Van, 1999). Although researches on climate change impacts develop fast, the links between hydro-climate and riparian ecosystem behavior (e.g. lakes, wetlands, fauna and flora) remain insufficient. Vegetation projections are uncertain partly due to incomplete knowledge on key variables. The understanding is hampered by the fundamental non-linear characteristic of climatic-hydro-ecological systems (MacDonald and Sertorio, 1990). An assumption underpinning this study is that an evaluation of climate change and its induced river flow variation will be a good starting point to study possible future changes of riparian vegetation. Moreover, climate conditions and water resources in the region are two important issues in ecosystem management and socio-economic development (Glantz, 2009).

One of the largest fluvial water bodies (in both length and volume) in Central Asia's water system is the Amu Darya River. The Amu Darya River Basin (ADRB) is located in the southern part of the Aral Sea Drainage Basin (ASDB). In this study, the ADRB offers a suitable site to investigate the response of river flow to the climate parameters in a basin scale. Narrowing down the basin scale to the scale of the Amu Darya River Delta (ADRD) is useful for examining the changes of river flow locally. This delta is vital to the Large Aral Sea's water budget, the livelihood in Uzbekistan and Turkmenistan, as well as the surrounding riparian ecosystem status (Asarin et al., 2009). Moreover, the locally unique riparian vegetation community in Central Asia is regarded as an ecological indictor to evaluate the effects of the changing hydro-climate conditions on the riparian ecosystem in the ADRD. Hydro-climate driven riparian vegetation change processes at basin scale may be important for understanding of ecosystem responses to climate change.

The purpose of this study is summarized as followed:

(1) To investigate dynamics between multi-GCM projections of future climate changes and hydrological variations in Central Asia;

(2) To study the implications of possible future changes in hydro-climate and river flow for a key riparian vegetation species in Amu Darya River Delta (ADRD), Central Asia;

(3) To examine uncertainties in projected river flow and locally created water flux.

The following section provides a detailed description of the study site (in **Chapter 2)**, including the characteristics of climate, hydrology, landscape and riparian ecosystem from large regional scales (i.e. Central Asia, the ASDB and the ADRB) and local scale (i.e. the ADRD). **Chapter 3** displays a conceptual framework used in this study in the beginning and then introduces details of the methodologies employed in four sub-sections. **Chapter 4** shows the results from this study and it starts from giving the present hydro-climatic conditions of the basin in **Section 4.1**. **Section 4.2** presents the outputs of climate change from multiple GCM projections and the interpretation of the uncertainties for different time period in studied region. In **Section 4.3**, the modeled spatially distributed evapotranspiration (ET) and the water flux (i.e. precipitation surplus, PS) as well as the accumulated river surface flow (R) are used to examine the hydrological responses in the ASDB and the ADRD under different plausible climate change scenarios. **Section 4.4** investigates the suitability of one key local riparian vegetation species via a qualitative analysis approach. The suitability synthesis helps to analyze the responses of this species under changing hydro-climate. Furthermore, **Chapter 5** discuses the results of this study in following aspects: (i) the hydro-climatic dynamics and projections in regional and local contexts, (ii) the uncertainty of GCMs driven hydro-climatic projections, and (iii) ecological management alternatives in the Amu Darya River Delta. Finally, **Chapter 6** gives a brief summary of findings in this study.

2. Study Site

2.1 The Aral Sea Drainage Basin

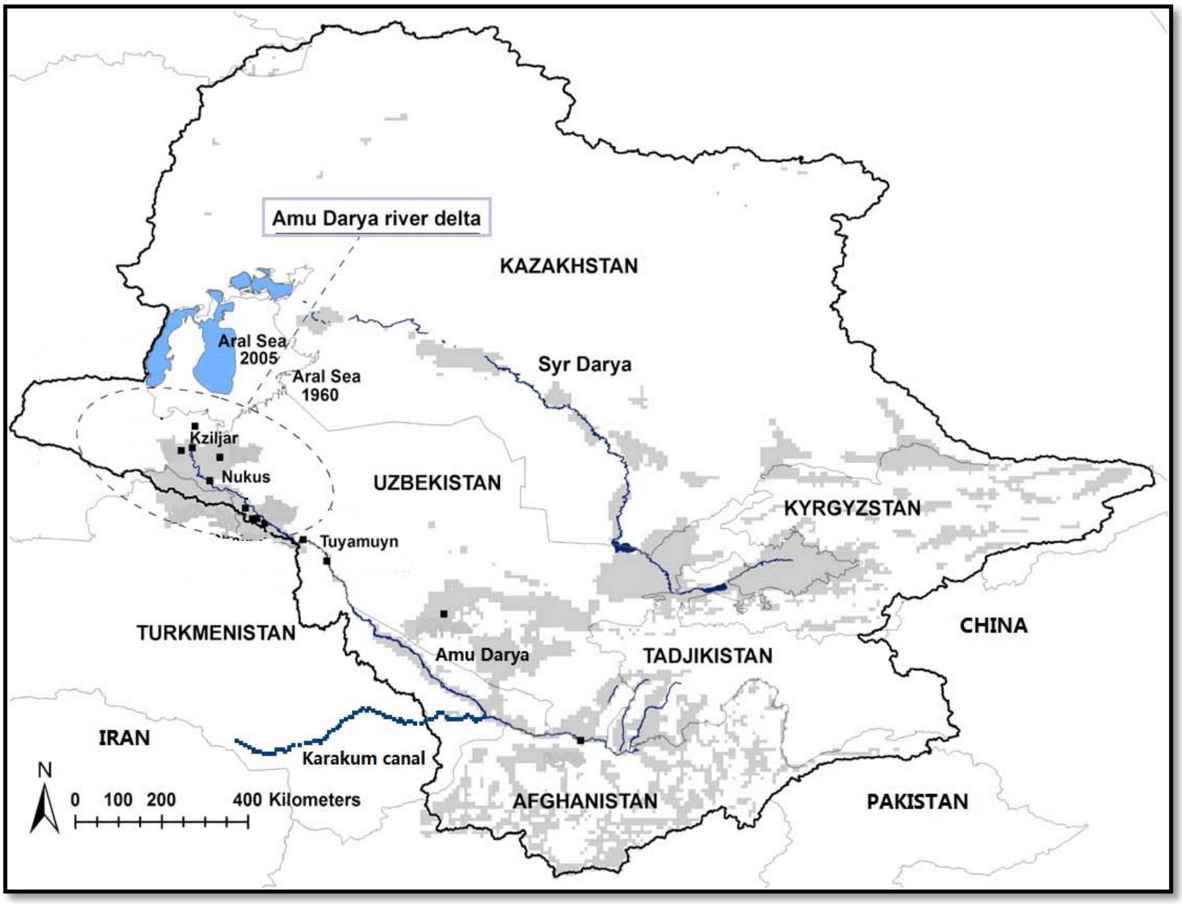

***Fig. 1** The map of the Aral Sea Drainage Basin (ASDB; in black solid line) located in Kazakhstan, Kyrgyzstan, Tadjikistan, Afghanistan, Turkmenistan and Uzbekistan, and with indicated extent of the Aral Sea in 2005 (in filled blue block) before its shrinkage and extend of it in1960 (in solid grey line) are shown. The Amu Darya, Syr Darya rivers (in solid blue lines) and the constructed Karakum canal (in dashed blue line) are the main irrigation water source exports to the irrigated areas inside (in grey areas) and outside the ASDB. The Amu Darya river delta (in dashed grey circle) is given ranging from the Tuyamuyn down to the river mouth connected to the Aral Sea. Source: Modified by Törnqvist et al. (2011) and Shibuo et al. (2007)*

The studied Aral Sea Drainage Basin (ASDB) occupies a large part of the Central Asia and covers 1.87 million km^2 (i.e. 1.3% of the earth's land surface) with six countries (Uzbekistan, Turkmenistan, Kazakhstan, Afghanistan, Tajikistan and Kyrgyzstan) (*Fig.1*) (Shibuo et al., 2007; Sorrel, et al., 2007; Törnqvist et al., 2011). The endorheic ASDB has an arid continental and semi-arid climate with extreme temporal and spatial variation of precipitation and temperature owning to its broadly variable topographical, geological and geographical structures (Lioubimtseva et al., 2005, Jarsjö and Törnqvist, 2010b). Four distinct seasons create vast fluctuations in temperature over the course of a year, and the extreme temperature reaches -30°C in winter and 45°C in summer (Asarin et al., 2009; Lioubimtseva et al., 2005). The precipitation is largest during spring but is generally scant all over the year (Sorrel, et al., 2007). The annual potential evaporation is higher than precipitations in most of the ASDB except for the mountainous region (Törnqvist et al., 2011).

Two major Central Asian rivers, the Syr Darya and the Amu Darya, feed most of the inland lakes, like the Aral Sea. 67% of the integrated renewable water in the ASDB is contributed by stream water from two rivers (*Fig.1*) (Glantz, 2005, Jarsjö and Törnqvist, 2010a). Moreover, water is a strategic and valuable natural resource in all arid Central Asia countries, not least because it sustains the region's economies with agriculture, particularly cotton production, accounting for approximately 20 ~ 35% of GDPs for countries within (Qi and Kulmatov, 2008; Micklin, 2002). Records show that the irrigated fields in the ASDB increase rapidly from 2.5 million hectares (ha) in 1910 to 7.4 million ha (i.e. occupy 75% of the area) in 1990 (Kulmatov, 2009; Jarsjö and Törnqvist, 2010b). More than 90% of the total river runoff in the downstream regions is currently diverted to irrigated fields via manmade irrigation canals (Cai et al., 2003). The largest manmade water diversion system, Karakum canal, was constructed in mid-1950s with a length of nearly 1300 km (can be found in *Fig.1)*. It diverts large amount of water from mid-reach of the Amu Darya in Uzbekistan to Turkmenistan (Glantz, 2005; Asarin, et al., 2009; Shibuo, et al., 2007). Overuse of water has lead to serious changes of the hydrological regime, which are associated with an array of severe environmental degradation in the surrounding regions, ranging from the degeneration of water resources, terrestrial and aquatic ecosystems to deterioration of human health and welfare (Micklin, 2004).

2.2 The Amu Darya River Basin

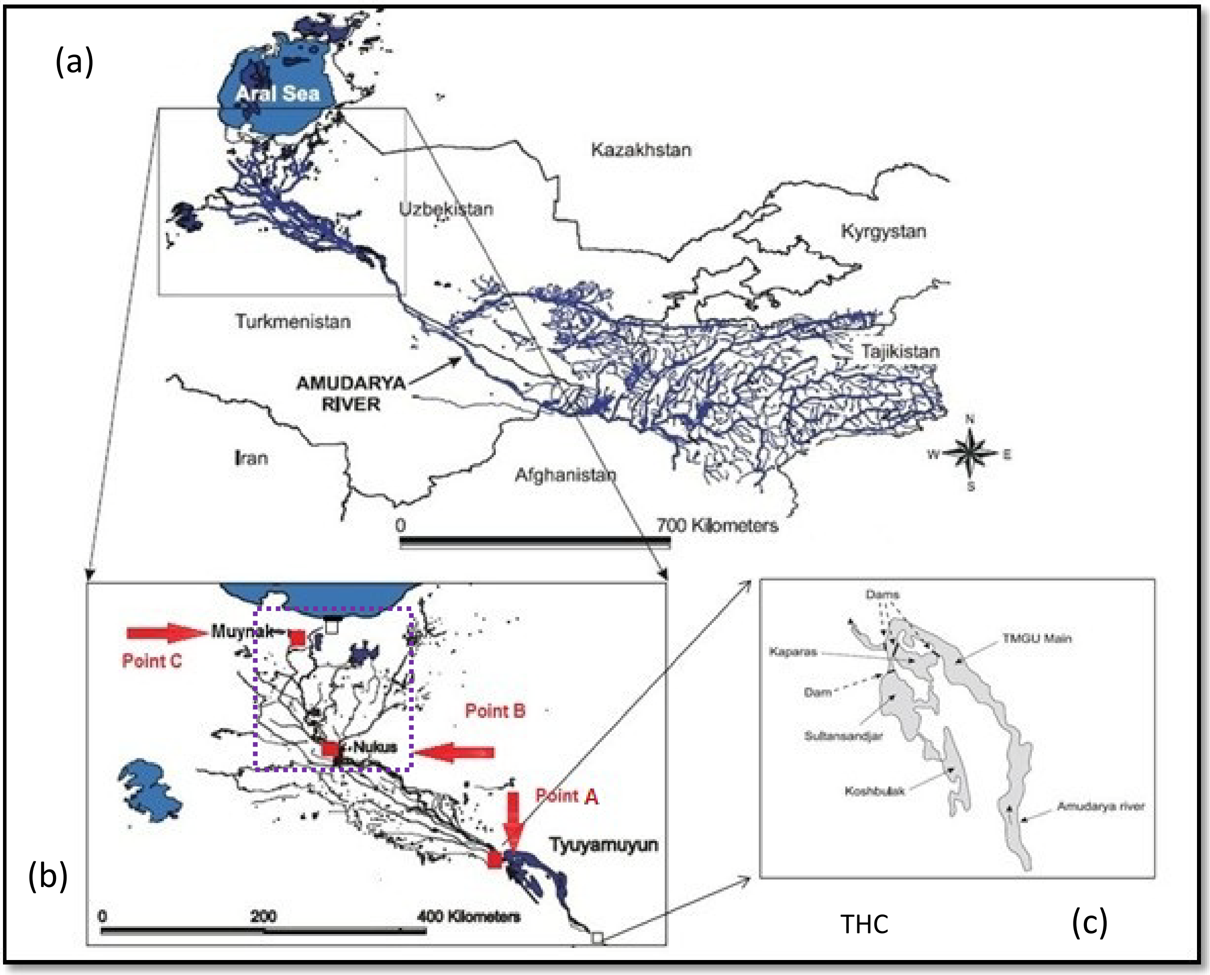

***Fig. 2** The top map (a) is Amu Darya River Basin (ADRB) comprises five countries and river drains into the Large Aral Sea. The natural Amu Darya River Delta (ADRD) (in map (a) with solid rectangle) indicates) is from the THC downstream till the Aral Sea. The enlarged map (b) within dashed rectangle displays the lower delta which mainly lies within the Republic of Uzbekistan in the Autonomous Republic of Karakalpkstan while only a small part (detail in Fig.3b) belongs to Turkmenistan stretching from Nukus to Muynak (i.e. the former port of the Aral Sea)(Rüger et al., 2003). The locations along the river (in the red solid square) are the studied sites. The enlarged map (c) shows the detailed scheme of the Tyuyamuyun Hydrologineering Complex (THC) at the inflow section to the ADRD. Source: Modified by Schlüter, et al., 2005 and Rüger et al., 2003*

The Amu Darya River Basin (ADRB), located within the ASDB, is the largest river basin in Central Asia, covering approximately 465,000 km^2 (*Fig.2a*) (Asarin et al., 2009; Glantz, 2005). The meltwater from snow and glaciers in the Pamir Mountains upstream is an important source for the river discharge (Glantz, 2009; Zonn et al., 2009). The Amu Darya River flows nearly 2540 km from its headwaters in Tajikistan passing Afghanistan, across the Karakum (i.e. Qyzylqum) desert entering Uzbekistan where it reaches the Tyuyamuyun Hydroengineering Complex (THC), by the THC flowing into the Amu Darya River Delta (ADRD) and eventually discharging to the shrinking Aral Sea (*Fig.1; Fig.2a,c*) (Glantz, 2009; Asarin et al., 2009; Froebrich and Kayumov, 2004).

Before the 1960s, the annual 79 km^3 river discharge through the Amu Darya delta to the Aral Sea was not only providing surface water but also feeding the groundwater system when the mean annual precipitation is about 100 mm or less, the groundwater recharge is negligible. Floods occurred every spring flushing the delta (Froebrich and Kayumov, 2004; Rüger et al., 2003; Micklin, 2004). Since 1980, as a result of the large-scale irrigation expansion in the ADRB as well as the regulation of river by the THC, average annual discharge dropped down to less than 10 km^3 and the natural flooding regime has almost gone (Törnqvist et al., 2011; Crosa et al., 2006). The continuous decrease in river flow has extensively altered the diverse deltaic ecosystems in the ADRB, such as flora and fauna, lakes, pastures and riparian forests. The delta here once played an important role in supporting irrigated agriculture, animal husbandry, hunting and trapping, fishing, and harvesting of reeds for the livelihood (Schlüter et al., 2005; Micklin, 2004).

2.3 The Amu Darya River Delta

A part of this study concerns the Amu Darya River Delta (ADRD), which is situated in Uzbekistan and Turkmenistan and covers approximately 19 000 km^2 *(Fig.2a)*. It is located between THC in the south and the outlet of the Aral Sea in the north (Rüger et al., 2003; Froebrich and Kayumov, 2004). Geographically, the ADRD is characterized as Turan lowland (defined as "*the flat and low part in the northwest of Central Asia represented largely by sandy and clay deserts*") (Zonn et al., 2009). Specifically, the pre-mouth area (the areas with yellow color in *Fig.3 (2, 3)*) connects to the Aral Sea and contains its dried bottom. It is physically characterized by low productivity (on solonchak and saline sands) while as far as the western part links by the Ustyurt plateau (Schlüter et al., 2005; Zonn, et al., 2009). The upper part of the delta is surrounded by the Kyzylkum and the Karakum deserts, whilst most of the irrigated fields (for cotton, white durra, corn and rice) are situated at the middle part of the delta

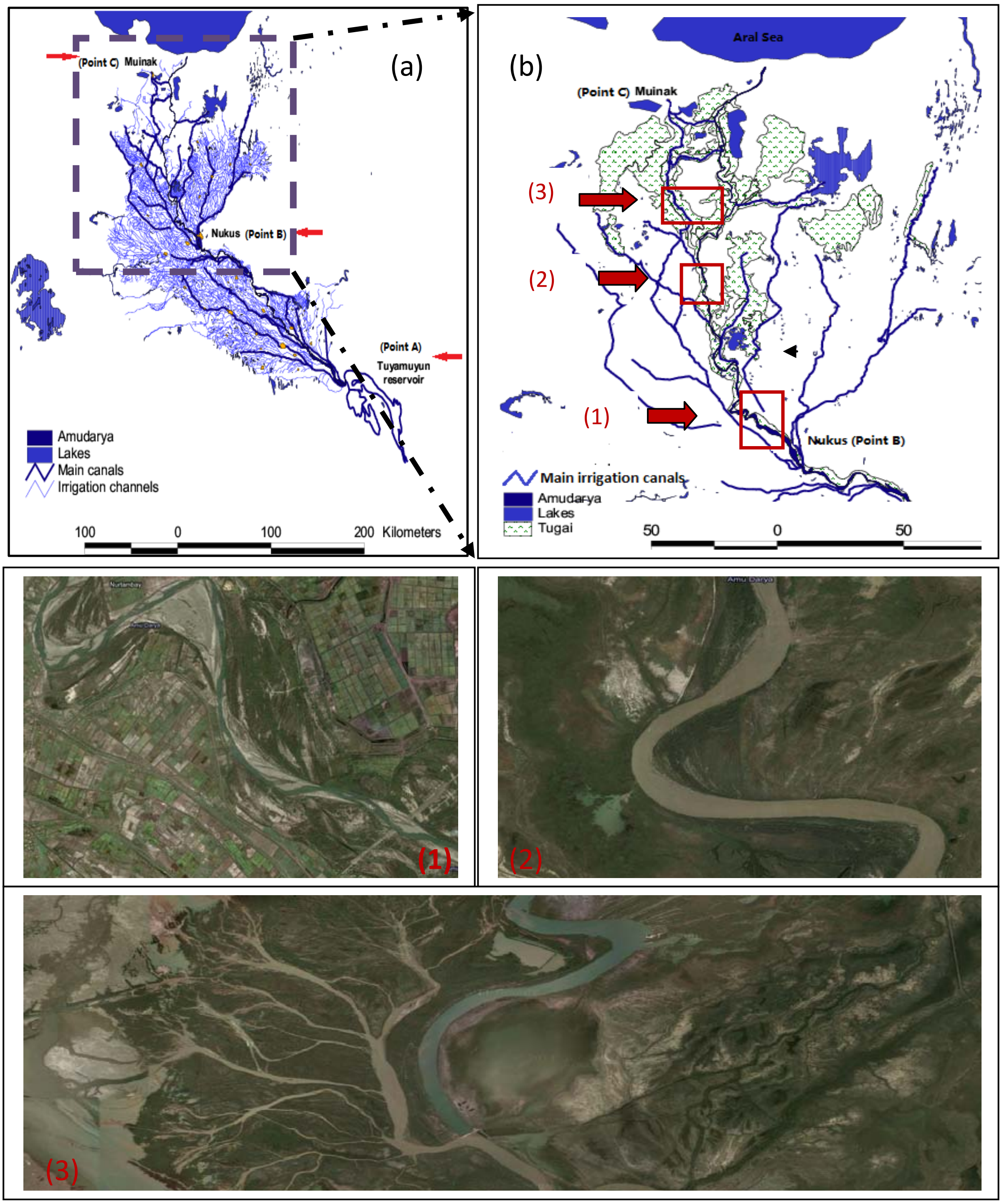

Fig.3 The map of lower reach of the Amu Darya River Delta in Fig. 3a (same as Fig.2b), the distribution map of Tugai forests in Fig.4b and the satellite image of landscapes for three locations with clear Tugai forests' belt (dark green part) along the rivers and canals display in Fig.3 (1.2.3). Source: Modified by Schlüter et al., 2003 and Google Map.

which takes up to approximately 876 000 ha (the intensive irrigated fields displayed as light green or yellow small squares in *Fig.3 (1))* (Rüger et al.**,** 2003; Schlüter et al., 2005; Törnqvist and Jarsjö, 2011; Asarin et al., 2009).

The landscape in the ADRD used to be covered by different types of ecosystems such as swamps, lakes, reed stands, and the typical riparian Tugai forests (e.g. poplar, tamarisk, and oak) (Rüger et al., 2003; Sorrel et al., 2003). One unique riparian vegetation community is Tugai, which defined as *"desertsilveta"* or *"Central Asian jungles"* and only occurs geographically in Central Asian, Middle Asian and Chinese arid steppes and lowlands. Tugai are living in river valleys and deltas of the regions as a narrow belt (which shows in dark green belt in *Fig.3(1,2,3)* and *Fig.3b* provides the distribution map of Tugai) (Micklin, 2004; Zonn et al., 2009; Rüger et al., 2003; Kuzmina and Treshkin, 1997). The special formations of Tugai communities are highly dependent on the hydrological regime (Treshkin et al., 1998). Severe alterations to the hydrological regime of the Amu Darya over the past 40 years have caused serious riparian ecosystem degradation in the lower ADRD and especially Tugai have suffered strong impacts in terms of species transitions and even extinction. According to the study of Novikova et al. (1998) Tugai covered 100,000 ha in the ADRD in 1950. However, by the 1970s the coverage was reduced to 52,000 ha, and by the mid-1990s only 15 ~ 20,000 ha was left. Tugai is important because they can prevent soil erosion and reserve water. Furthermore, they are also the important habitat for a diversity of animals, including 60 species of mammals, more than 300 types of birds and 20 varieties of amphibians. Tugai hence provides important ecological services (e.g. formation of soil biomass, melioration of the microclimate and preservation of biodiversity) for the regions around (Rüger et al., 2003; Novikova et al., 2001).

2.4 Tugai community in the Amu Darya River Delta

There are 190 diverse Tugai species in the ADRD, who share the characteristics of having high capacity to tolerate drought, super wet soil, salts and very dry air (Zonn et al., 2009; Treshkin et al., 1998; Schlüter et al., 2005). The main Tugai species in the delta can be categorized into three formations: (1) the woody-bush Tugai grow as a dense gallery on the river alluvium. It can for instance contain poplars (*Populus euphratica)*, willows (*Salix songarica)*, saxaul *(Halimodendron halodendron, Haloxylon)* (*Fig.4a*); (2) the fringe bush Tugai containing mainly salt cedar (*Tamarix ramosissima)* and liquorice *(Glycyrrhiza glabra)* are typically located at some distance from the river bank where the groundwater

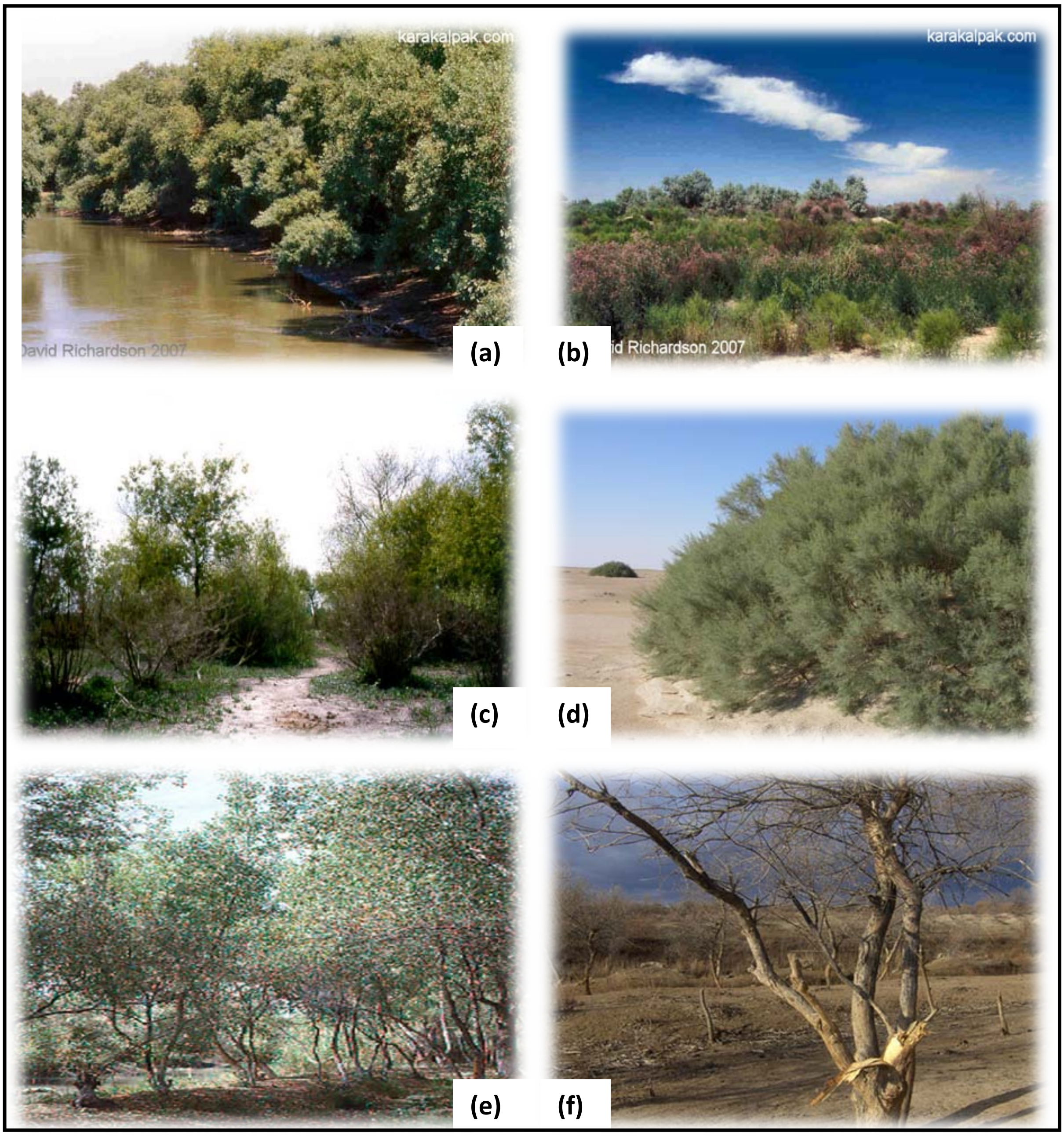

Fig.4 Tugai communities grow along Amu Darya River Delta. Photos display different conditions and formations of Tugai. Photo (a) shows the small remnant of woody-bush Tugai along the Amu Darya River (Photo was taken in 2004 Uzbekistan). The fragment of bush Tugai with tamarisk and liquorice shows in photo (b). Trace of grass Tugai patch near Kyzyljar (Amu Darya delta) is shown in photo (c). Photo (d) display the scene of the Halostashys caspica in desert near the delta. Photos (e,f) display the scenes of the healthy (e) and degraded (f) Tugai communities growing in the Amu Darya River Delta. Sources: http://karakalpak.com/stangeography.html http://www.plantarium.ru/page/image/id/40320.html, Schlüter et al., 2005, and Rüger et al., 2003.

table is relatively low and the soil salinity is relatively high (*Fig.4b*); (3) the grass Tugai dominated by *Halostachys caspica* that grow further away from the river bank and even extent to the desert (*Fig.4c*, *d*)

(Rüger et al.**,** 2003; Zonn et al., 2009; Schlüter et al., 2005). Changes in groundwater level, soil salinity, distance to surface water to large extent determine Tugai communities' condition (as *Fig.4e, f)* shown both healthy and degraded Tugai. Three categories of Tugai maintain the richness and integrity of the communities' structure.

3. Materials and Methods

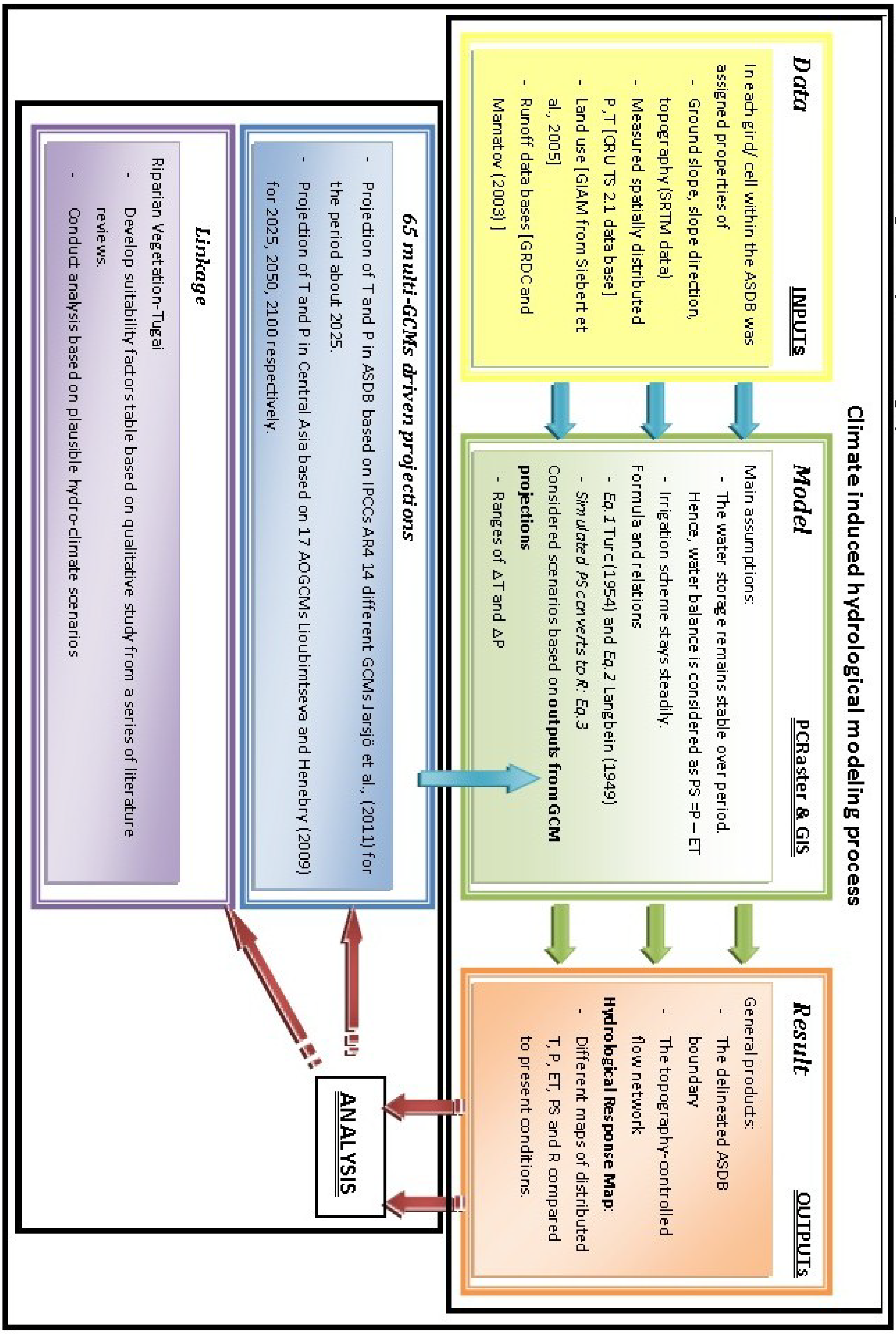

Fig. 5 The conceptual framework of this study, which includes: hydrological modelling process (the data required as the input for the model and the assumptions made, formula and relations used, hypothetical scenarios designed to operate the model and the expected outputs from the model) and two analysis aspects according to the outputs from the mode in the light of partly with the multi-GCMs driven projections (on bottom left)and partially with the interaction between vegetation (on bottom right).

Fig.5 shows schematically the methodological framework of this study, including also how data, models, results, and analyses are integrated in a logical way. The boxes of *Fig.5* are connected by arrows in different colors, which conceptualize certain relationships or functions between one box and another box. For instance, the blue arrows represent the step of providing useful data to the model; the green arrows stand for outcomes produced by the model as results of the study; and the red arrows represent analyses that are made on the basis of the modeling results. Specifically, the upper part of *Fig.5* shows that the climate-driven hydrological modeling is performed in the three main steps (shown as yellow, green and red boxes in *Fig.5*) of data processing, quantitative modeling, and output processing, which will be explained in detail below in **Section 3.2** and **Section 3.3**. The centered blue box in *Fig.5* is regarded as one part of the inputs to the model and also provides a basis for conducting robust analysis in investigating relationship with results from other boxes (detailed explanations of this box could be found in **Section 3.1**). The bottom purple box and the red arrows show that the results from the hydrological modeling step are used as reference to analyze the linkages between riparian vegetation and hydro-climatic conditions under the changing climate projections, which will be interpreted in **Section 3.4**. The conceptual model of *Fig.5* can more generally be regarded as a framework of this study.

3.1 The multi-GCM projections of future hydro-climatic changes

So far, forecasts of anthropogenic and natural climate change have been associated with large uncertainties, so that scenarios of future climate conditions have been developed to provide quantitative assessments of the hydrological consequences in the river basins. Global climate change projections are available from a series of GCMs under the IPCC GHGs emission scenarios, which use as input narrative storylines on future CO_2 emission. The GCMs provide useful information on climatic variations in different part of the world. In this study, we investigate the outputs of T and P from 65 GCMs projections' changes (△T and △P) since the reference period 1961~1990 partially for the Central Asia and partly for the ASDB. The considered △T and △P values were previously produced in two studies done by Jarsjö et al., (2011) and Lioubimtseva and Henebry (2009). Since the surface of the basin covers a reasonable number of GCM grid cells, these studies used GCMs instead of regional climate models (RCMs) to produce climate change projections of the considered areas. One ensemble of projections (referred as P1) of △T and △P between the period 2010 ~ 2039 (i.e. around 2025) and the reference period 1961~1990 for the ASDB was studied by Jarsjö et al. (2011). These projections are based on IPCCs AR4 of 14 different GCMs, i.e. CSIRO-CSMK3, ECHAM5-MPEH5, GFDL-GFCM_20_21, HADCM3, NIES-MIMR, CNCM3, ECHOG, GIER, HADGEM, INCM3, IPCM4, MRCGCM, NCCCSM, NCPCM, CSIRO-MK2, ECHAM4, GFDL99-R30, HADCM3, CCSR-NIES and CCCma-CGCM2. The rest of projections, which regard differences between the individual years of 2025, 2050, 2100 (referred as P2, P3, P4) and reference year 1961~1990, are based on 17 different GCMs (i.e. UIUC-EQ, CSIRO2-EQ, NCAR-DOE, CSIRO1-EQ, GFDK-TR, BMRC-EQ, HadCM2, CSIRO-TR, ECHAM1, CCSR-NIES, ECHAM3, CCC-EQ, ECHAM4, UKHI-EQ, CGCM1-TR, UKTR, ECHAM5) for Central Asia, and were reported in the study of Lioubimtseva and Henebry (2009).

The above studies hence yield 65 different pairs of projected △T and △P change (14 pairs from the study of Jarsjö et al., (2011) plus 17 times 3 pairs from the study of Lioubimtseva and Henebry (2009) that considered three different representative years). For a given study and four projection envelopes (P1, P2, P3, P4), a total projection envelope can be defined from the full range of (△T and △P) results. Hence, four projection envelopes can be distinguished corresponding to the three different time periods of the Lioubimtseva and Henebry (2009) study and the time period of the Jarsjö et al., (2011) study, which overlaps with the first period of Lioubimtseva and Henebry (2009) study. Furthermore, the four projection envelopes can be further categorized into three different time windows: near future (S-window, referring to the time period around 2025, i.e. obtained from P1 and P2), mid century (M-window, referring to the time period around 2050, i.e. P3) and distant future (L-window, referring to the time period around 2100, i.e. P4). These three different time windows assist to evaluate the uncertainties in time. Moreover, this study encompasses a wide range of climate change scenarios for both near and distant future time windows (i.e. S-window and L-window). Thus, the low ends and the high ends from the ranges of S-window and L-window are regarded as one wet scenario and one dry scenario, which are selected to further simulate the corresponding spatial hydro-climatic changes in the modeling process (which will be explained in **Section 3.2**). Therefore, the range, the ensemble means (EM), the standard deviation (SD) and the coefficient of variation (CV) of each projection envelope (and each time window) are summarized to compare different scenarios. The results could be used as important references to estimate the potential impacts of climate change on hydrological system and also to investigate the uncertainties of hydro-climatic conditions for the study site.

3.2 Hydrological modeling

The PCRaster-based Pol-flow model is employed to fulfill the spatially distributed simulations for climate-driven hydrological change in the ASDB (De Wit, 2001). The study of Shibuo et al. (2007) provided a solid quantification basis for this study. They successfully modeled the past changes of water balance and hydrological cycles under anthropogenic and climatic pressures in the whole ASDB, using historical spatially distributed climatological data over last five decades (i.e. from 1983 to 2002). The model used in this study follows the similar procedures as in studied of Shibuo et al. (2007) and Jarsjö et al. (2011), and also is assigned properties in each of the 3000×3000 grid cells in the basin. Specifically, based on data from the Shuttle Rader Topography Mission (SRTM) (Farr et al., 2007), the topographic-driven flow routes of the basin are generated according to the ground slope and slope direction (details referred to Jarsjö et al. (2011)). The climatic status of the annual averaged temperature (T) and precipitation (P) are based on measured data gained from the Climate Research Unit (CRU) TS 2.1 data base (Mitchell and Jones 2005). The data of irrigated areas are generally assigned to land use character of the ASDB, data are partly based on the Global Map of Irrigated Areas (GMIA) (Siebert et al., 2005) and are partly adopted from the study of Törnqvist and Jarsjö (2011). For the discharge of two rivers the Amu Darya and Syr Darya, the observed data is gained from the runoff data bases in Global Runoff Data Centre (GRDC) (Mamatov, 2003). These above mentioned input data are used for generating outputs in terms of spatially distributed maps regarding the evapotranspiration (ET), the precipitation surplus (PS, i.e. the difference between P, ET and changed storage, PS=P-ET-$\triangle$S), and the river flow (R, i.e. routed rivers accumulated by PS from upstream areas to downwards) (Shibuo et al., 2007; de Wit, 2001; Jarsjö et al., 2011). In this study, water balance calculations are used long term historical data to achieve, one assumption hence can be made is that assume the water storage remains stable. Namely, precipitation surplus could be expressed equivalently as the difference between P and ET (i.e. PS=P-ET), and also equivalent to the convergence of horizontal atmospheric water flux (Milly et al., 2005).

In order to estimate the actual evapotranspiration (ET) for this study, the empirical relationship developed by Turc (1954) is employed, which formulates the relation as a function (*Eq. (1)*) expressed by the actual evapotranspiration (ET in mm), precipitation (P in mm) and potential evapotranspiration (ET_p in mm).

$$ET = \frac{P}{\sqrt{(0.9 + \frac{P^2}{ET_P^2})}} \qquad Eq.\ (1)$$

The ET_p can be further estimated by another empirical relationship according to Langbein (1949). Specifically, the ET_p is formulated as a function (*Eq. (2)*) by annual temperature (T in °C) and the parametric constants.

$$ET_P = 325 + (21 \times T) + (0.9 \times T^2) \qquad Eq.\ (2)$$

In *Eq. (1)* and *Eq. (2),* the parametric constants have appropriate associated units and account only implicitly for the effects of soil and vegetation on potential and actual evapotranspiration, which may bring out certain errors for ET (in mm) in different landscape (De Wit, 2001). This study will not include this kind of model uncertainty in the uncertainty analysis.

After calculating PS based on water balance for all grid cells, add neighboring PS cells into the river networks and accumulate from upstream to downstream step by step, and then flowing the water in the cells to the river mouth to get the accumulated discharge (R in mm/year). This process artificially simulates the river stream and coastline in a simple way. Besides, the accumulated discharge can be characterized by PS and the cell areas (A) as:

$$\sum R = \sum[PS \times A] \ or \sum R = \sum[(P - ET) \times A] \qquad Eq. (3)$$

Therein, the cell areas, A, were calculated for different latitudes, thereby accounting for effects of the earth's curvature (Shibuo et al., 2007). Additionally, not only consider the large-scale irrigated land as landscape property but also account the water diverting from river to largest human made irrigation canal, Karakum canal, as one strongest anthropogenic effect in this region to the hydrological condition. Explicitly, consider the superficial nature of the ASDB irrigation water by adding its contribution as extra P over the irrigated land, which regard the Karakum canal as a sink to be able to get the actual river discharge along the river coast (for details which can be referred to Shibuo et al., (2007)).

This study initially attempts to produce today's spatially distributed hydro-climatic condition in terms of T, P, ET, PS and R. The current hydro-climatic conditions for T, P, ET, PS and R are expressed as T_0, P_0, $ET_{0,}$ PS_0 and $R_{0,}$ which are regarded as baseline for following hydro-climatic changes. The above mentioned (in **Section 3.1**) wet scenarios and dry scenarios with corresponding △T and △P values for the S-window (around 2025) and the L-window (around 2100) are then used as inputs to generate basin-scale spatially distributed maps of changed ET (△ET) and changed PS (△PS). Specifically, △ET is equivalent to the modeled ET subtracted by the current ET values (i.e. $\triangle ET = ET_{(modeled)} - ET_0$), while △PS is equivalent to modeled PS subtracted by PS_0, (i.e. $\triangle PS = PS_{(modeled)} - PS_0$).

To examine the variations of river flow in the delta resulting by climate change under current irrigation schemes, both ⊿R (i.e. $\triangle R = R_{(modeled)} - R_0$) and the absolute R are quantified. Three sites in the delta, Point A, B and C of *Fig.2* and *Fig.3* are selected for this purpose. Additionally, the current hydrological regime in the delta is to large extent determined by the irrigation withdrawals in the upper, middle and lower reaches of delta. Therefore, the analysis of the flow behavior change in absolute quantification should also consider the different extent of irrigation withdrawals (Q) in each segment of delta, consequently, there are large differences of river runoff in each studied point in delta (i.e. for the entire delta the annual water consumption for irrigation is 24.8 km^3 (Törnqvist and Jarsjö, 2011), expressed as $Q_A = 24.8 km^3$). However, the calculations of irrigation water use in other segment of delta are based on the fraction of irrigation areas in ADRB studied by Törnqvist and Jarsjö (2011) and the percentage of irrigation fields studied by Shibuo, et al. (2007) to calibrate the absolute river flow in each segment of the delta. Namely, use $R_{(absolute)} = R_{(modeled)} - Q$ to estimate the river flow from Point A, B, C, to the outlet and the volume of water withdraw are expressed as Q_A, Q_B and Q_C.

3.3 Hydrological Response Map

Table 1 The matrix of ΔT_i and ΔP_j for producing a hydrological response map.

ΔT_i / ΔP_j	$\Delta T_{(i=1)}$	$\Delta T_{(i=2)}$	…	…	…	…	ΔT_i
$\Delta P_{(j=1)}$	($T_0 + \Delta T_1$, $P_0 + \Delta P_1$)	…	…	…	…	…	($T_0 + \Delta T_i$, $P_0 + \Delta P_1$)
$\Delta P_{(j=2)}$	($T_0 + \Delta T_1$, $P_0 + \Delta P_2$)	…	…	…	…	…	($T_0 + \Delta T_i$, $P_0 + \Delta P_2$)
…	…	…	…	…	…	…	…
…	…	…	…	…	…	…	…
…	…	…	…	…	…	…	…
…	…	…	…	…	…	…	…
ΔP_j	($T_0 + \Delta T_1$, $P_0 + \Delta P_j$)	…	…	…	…	…	($T_0 + \Delta T_i$, $P_0 + \Delta P_j$)

A common way of adding hydrological modeling steps to GCM results is to use GCM outputs as direct inputs to the hydrological model. In the present study, this would mean running the hydrological model 65 times, each time using the paired ΔT and ΔP results from the considered 65 GCM mode runs as inputs (see **Section 3.1**). If several GCM models for instance would yield similar ΔT and ΔP outputs, this would mean that some hydrological model runs would give low amount of new information. In order to increase the information content of each hydrological model run, we here instead discretize the total prediction envelopes of $\triangle T$ and $\triangle P$ using even spacing, giving an array *i*j* nodes in *Table1*. Specifically, the first row of *Table1* shows that there are *i* evenly spaced nodes of $\triangle T$ while the first column shows *j* evenly spaced nodes of $\triangle P$. The double frame of *Table1* forms a matrix of the combinations of modeled future T and P, which is produced by adding the $\triangle T$, $\triangle P$ values to the observed historical baseline map of T_0 and P_0 mentioned in **Section 3.2** (i.e. $T_{(modeled)} = T_0 + \triangle T_i$ and $P_{(modeled)} = T_0 + \triangle T_j$). By running the modeling each time (the hydrological model described in **Section 3.2**), *i*j* values of $R_{(modeled)}$ are generated resulting by different combination of $\triangle T$ and $\triangle P$ in the matrix (i.e. each node of ($\triangle T_i$, $\triangle P_j$) in *Table1*). Furthermore, in this study, the values of those nodes are interpolated to produce a continuous 'Hydrological Response Map', which could visualize the probable responses of river flow to climate changes.

3.4 Riparian vegetation qualitative analysis approach

In order to analyze the response of one key species among riparian vegetation to the changing hydro-climatic conditions for different time periods in the ADRD, the initiative step is to investigate the suitability of this species from multiple factors. Therefore, qualitative approach is employed to examine the suitability and optimal living status, referring a series of studies. The hydro-climate related influence factors are directly derived from several studies done by Rüger et al. (2003), Treshkin (2001), Novikova et al. (2001), Kuzmina and Treshkin (1997), Ma et al. (1997), Bakhiev and Treshkin (1991) and Schüter et al. (2005). By synthesizing relevant hydro-climatic influence factors together, it could provide as one reference to further evaluate the plant conditions under studied probable hydro-climate scenarios in terms of formation, development, transformation, diversity, degradation, etc.

4. Results

4.1 Current hydro-climatic conditions

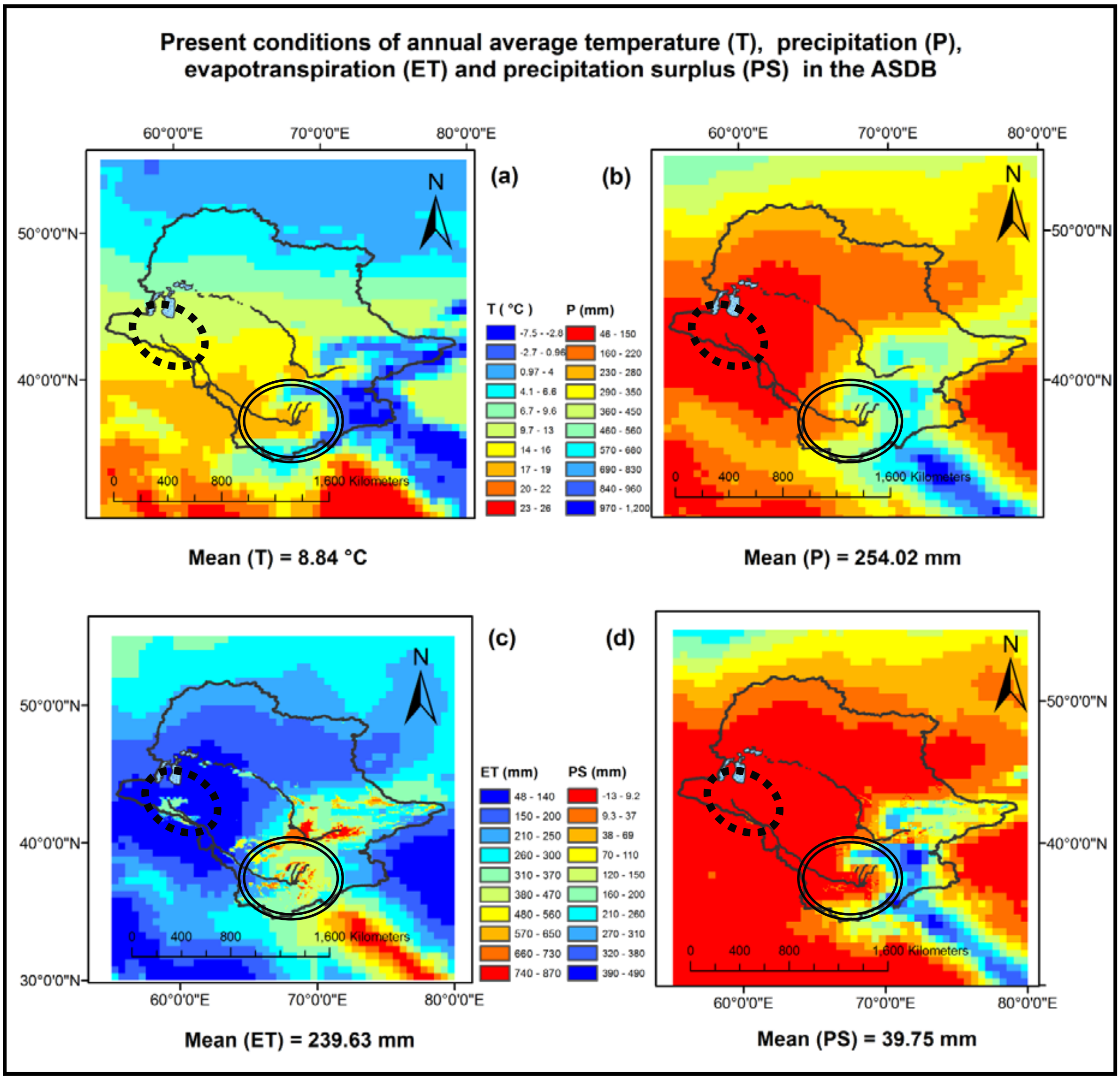

***Fig.6** The distributed maps of present annual average T and P based on observational data are shown in the top (a and b), and the maps of the modeled absolute ET and PS based on calculations are given in the bottom (c and d). Furthermore, the annual mean (EM) of each variable within the whole ASDB (solid black line is the boundary of basin) are estimated and given below each map. The delta of Amu Darya is marked by dash black circle in each map while the upstream region is highlighted by solid double lines ellipse in each map. The irrigated fields refer to Fig. 1 (the grey shadowed area).*

Before investigating the future changes in the climatology of T and P and their associated hydrological regime variations, *Fig.6* summarizes the present ASDB hydro-climatic conditions in terms of T and P, ET and PS. The spatial distribution maps not only provide the basic spatially distributed hydro-climatic characteristics of the basin but also give a baseline for a comparison with projections. The general message gained from *Fig.6* is that the climate with its large spatial variations of T, P and ET shows a strongly heterogeneous pattern, especially comparing the upstream (eastern region) with the downstream (western region) of the ADRB.

Specifically, the upstream region holds a climate with low average annual T (7°C) and high P (450 mm) relative to the means of the whole basin (*Fig.6a,b* gives the mean values of T and P below each map of roughly 9°C and 250 mm). The mean upstream ET of 360 mm/year is also (like P) much higher than the average value of the whole basin (*Fig.6c*). The downstream ADRD hence holds a rather high T and low P, with annual averages 13 °C and 95 mm respectively (*Fig.6a,b*). However, the upper and middle reach of the delta region (from Tyuyamuyun to Kziljar) has also a higher annual ET (with 330 mm) compared to the mean ET (of 240 mm), while the lower reach delta region, from Kziljar to the outlet of Aral Sea, has a lower ET (130 mm) than mean ET and the ET at other locations of delta (*Fig.6c*). Therefore, according to *Fig.6d*, the mean modeled PS (namely, the remaining water in each grid cell in the basin) is negative (-2 mm) in the downstream delta and has a relatively large positive value (330 mm) in the upstream, which clearly demonstrates that water resources in the downstream delta are highly dependent on the upstream region for generating runoff.

4.2 The changing regional climate

Fig.7 summarized the $\triangle$T and $\triangle$P from four projection envelopes and *Table2* supplements some specific values for range, EM, SD and CV of $\triangle$T and $\triangle$P. The two prediction envelopes for the near future conditions around 2025 (i.e. P1 and P2 with the blue and purple rectangular envelopes respectively) largely overlaps and indicates that the $\triangle$T of the ASDB will be between approximately 1°C to 2°C. By contrast, the predicted near future (around 2025) $\triangle$P in this region gives a relatively large range from a decrease of 16 mm/year (i.e.-6 %) to an increase of 26 mm/year (i.e. 10%) (*Fig.7; Table2*).

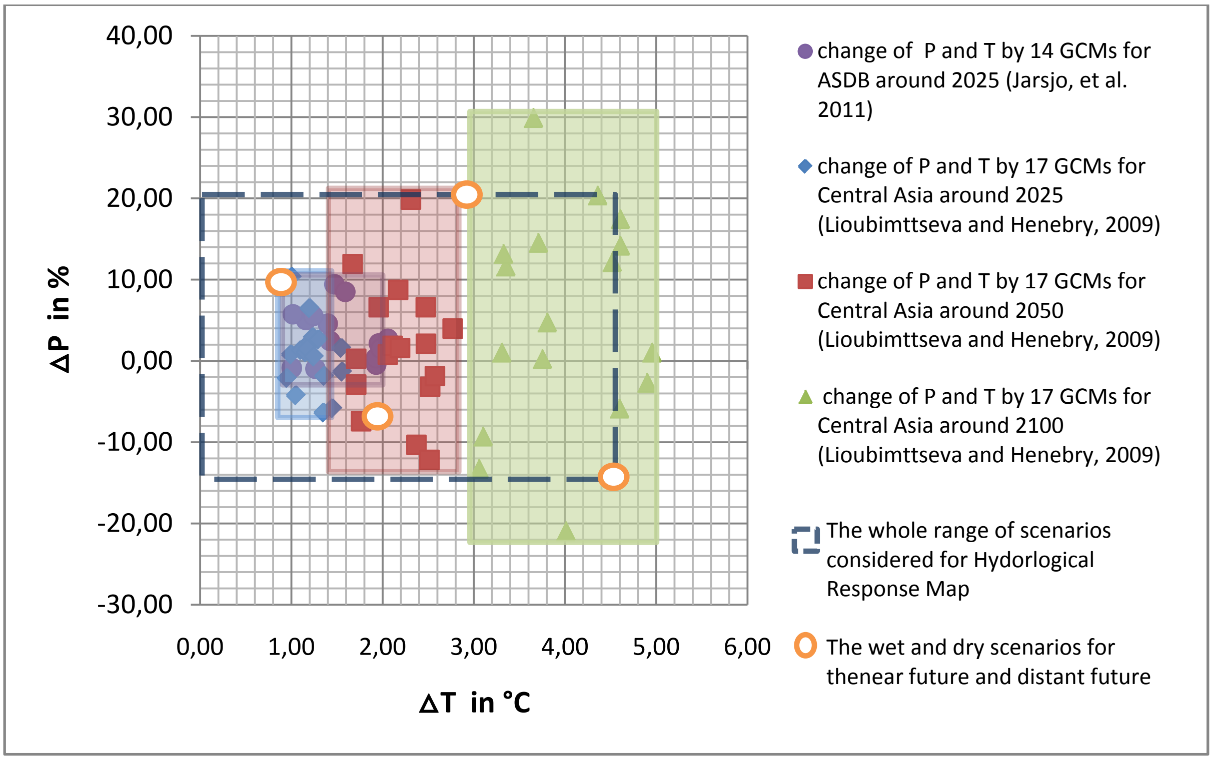

Fig.7 The future predictions of climate change in the ASDB according to multiple GCMs operated by two studies for different time and space. The purple dots (P1) are the symbols of possible climate change projection for P and T over the ASDB according to 14 GCMs around 2025, which are studied by Jarsjö et al. (2011). Conversely, the blue (P2), red (P3), green(P4) dots respectively represent the probable predictions of P and T based on 17 GCMs for Central Asia in different time scales, which are made by Lioubimttseva and Henebry in 2009. The colored solid rectangle circled the each colored dots' spread stands for the envelope of each future projection for near future (S-window)(i.e. blue and purple rectangles), mid century (M -window)(i.e. red rectangle) and distant future (L-window)(i.e. green rectangle) respectively. All considered scenarios for the Hydrological Response Map show as the hollow dashed rectangle in the figure and the dry or wet scenarios within range are drew down with four yellow points only for near future and distant future.

Overall, the EM value in total 31 different GCM results for near future's ΔT and ΔP illustrates an increase of 1.4°C and 5.0 mm/year (2%) respectively (average value of first two columns in *Table2*). For the period of mid-century (around 2050), ΔT is expected to further increase to roughly 2.2 (1.7 ~ 2.8)°C (see the M-window; pink rectangular envelope of P3 in *Fig.7*), whereas the ΔP projections show a larger spread (from - 31 mm to 51 mm, i.e. from -12 % to 20 %) with however an increase in mean ΔP of 4 mm (i.e.1.6%) which is similar to the near future projection EM of ΔP (4.9 mm or 2 %). The L-window (green rectangular P4 envelope) in *Fig.7* shows that ΔT is projected to increase to 3 ~ 5°C around 2100. However, the spread of ΔP is large (from -53 mm to 76 mm; from -21% to 30%), demonstrating △P projections are relatively uncertain for distant future. The ensemble mean △P is 13 mm (5 %) per year in L-window. In summary, the projections become increasingly uncertain for both △T and △P in time according to the gradually increased surface of the projection envelopes in *Fig.7*.

Table2 The change of temperature and precipitation under each GCMs' prediction envelopes, showing by the ranges, ensemble means, standard deviations, coefficient of variation in details for different time windows.

Time Window	**Near future (S)**		**Mid century (M)**	**Distant future (L)**
Projection envelope	**P1**	**P2**	**P3**	**P4**
Time scale	2025	2025	2050	2100
No. of GCMs	14GCMs	17GCMs	17GCMs	17GCMs
Range of △T (°C)	1.00 ~ 2.06	0.950 ~ 1.56	1.67 ~ 2.77	3.05 ~ 4.95
EM of △T (°C)	1.53	1.23	2.20	3.97
△T 's (SD) [CV] **(°C)	(0.380) [0.250]	(0.180) [0.150]	(0.340) [0.150]	(0.640) [0.160]
Range of △ P (%) *	-0.970 ~ 9.44	-6.36 ~ 10.3	-12.2 ~ 19.9	-20.9 ~ 29.9
Range of △P (mm) *	-2.46 ~ 24.0	-16.2 ~ 26.2	-31.0 ~ 50.5	-53.2 ~ 76.0
EM of △T (%/mm)	3.27/8.31	0.580/1.47	1.56/3.96	5.23/13.28
△P's (SD) [CV] ** (%)	(3.33) [1.00]	(4.15) [7.16]	(7.98) [5.12]	(13.2) [2.53]

* The positive values mean the increasing directions while the negative values indicate the decreasing trends. And the values are given in two units with % and mm respectively.

** The standard deviation (SD) shows in parenthesis whilst the coefficient of variation [CV] displays in square brackets. For P, table gives the increased EM for P in two units with % and mm respectively separating by slash (/).

The here considered ranges of △T and △P were obtained considering the projections envelopes of the P1, P2, P3 and P4 GCM results. *Fig.7* also shows the overall coverage of △T and △P, as expressed by the hollow dashed rectangle. The values of △T and △P is a matrix of climate change projection, △T is ranging from 0°C to 4.5°C and △P is ranging from -15% (- 33 mm) to 20 % (50 mm). Besides, increasing 1°C/2°C for △T and increasing 10% (25 mm) / decreasing 5% (13 mm) for △P are set up for wet-scenario/ dry-scenario in near future (see the yellow hollow points in *Fig.7*). In analogy, wet-scenario and dry-scenario for distant future are regarded as △T increases 3°C, △P increases 20% (50 mm) and △T increases 4.5 °C, △P decreases 15 (38 mm) respectively (*Fig.7*).

4.3 Results of different hydrological conditions under different climatic scenarios

4.3.1 Modeled changes of ET and PS conditions under plausible climate scenario

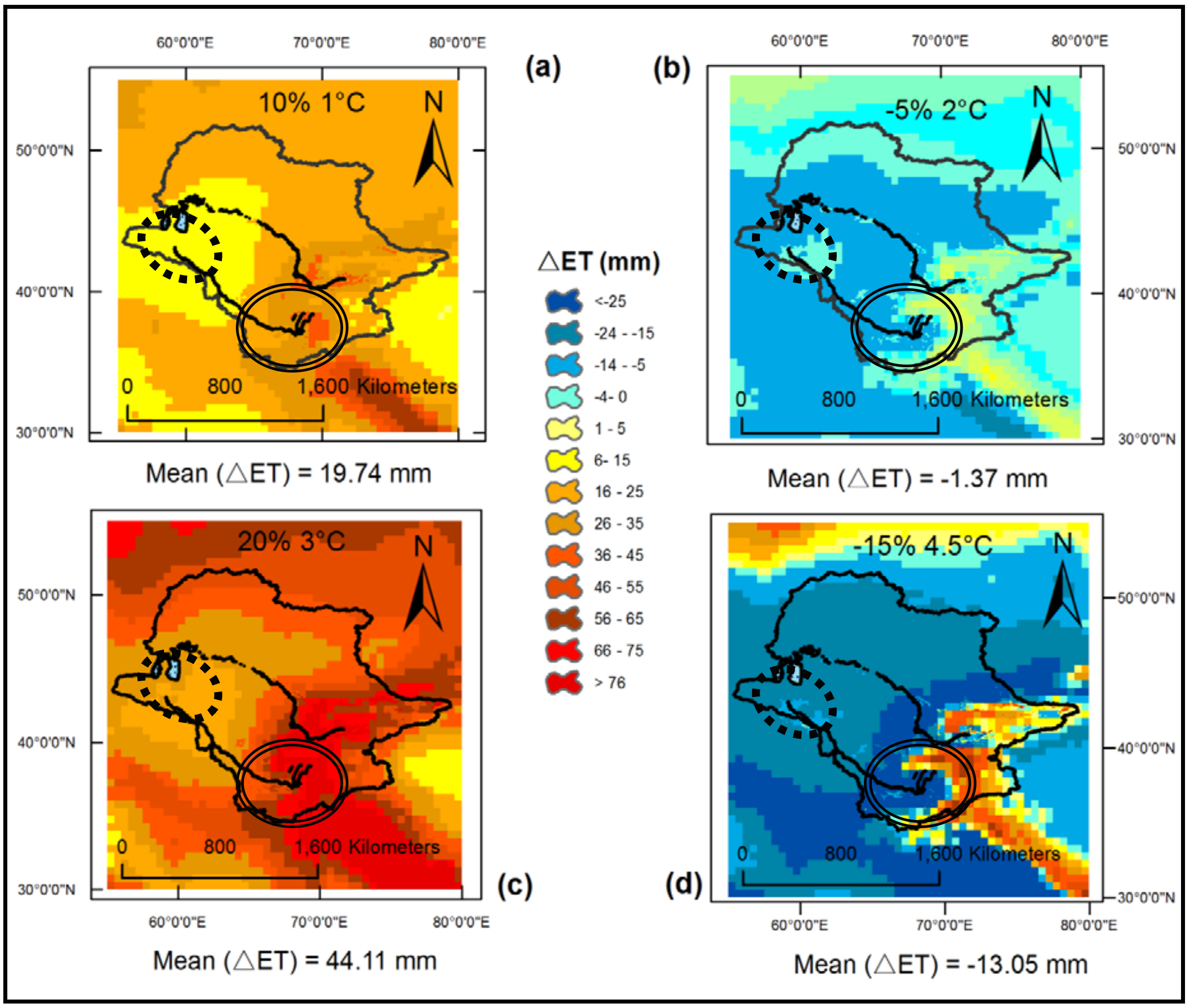

Fig.8 ***The modeled ΔET under four scenarios for near future (top two maps) and distant future (bottom two maps) predictions are showed in (a), (b); (c), (d) respectively. Two left maps are wet scenarios while two right maps stand for dry scenarios for near future and distant future projections correspondently. These four scenarios correspond to the scenarios given in Fig.7 (with yellow points). Means of change within the whole ASDB (solid black line is the boundary of basin) are estimated and given below each map. The delta of Amu Darya is marked by dash black circle in each map while the upstream region is highlighted by solid double lines ellipse in each map.***

Fig.8 shows the simulated ΔET under wet scenarios and dry scenarios (in different columns) for period of around 2025 and around 2100 accordingly (in different rows). Specifically, under the wet scenario, ΔET is likely to increase across the whole basin in near future (*Fig.8a*) and in distant future (*Fig.8c*), while, the dry scenarios in *Fig.8b,d* display the opposite trends of △ET that may decrease in most regions of the basin except for upstream regions. Namely, once increasing △T and decreasing △P, the annual averaged △ET would increase accordingly, whereas, once △P increases even though △T still goes up, △ET will experience an increase.

Over the basin, the near future △ET is likely to increase 20 mm/year under the wet scenario (i.e. △T= 1°C and △P = 25 mm / 10%) while it may decrease 1 mm under the dry scenario (△T = 2°C and P = - 12 mm/ - 5%) (*Fig.8a, b*). The wide range of the two scenarios shows △ET has a large variation within the basin in the near future. In analogy, for the period around 2100 △ET may increase 44 mm under the wet scenario (T = 3°C and P = 50 mm/ 20%) and decrease 13 mm under the dry scenario (T = 4.5°C and P = - 38 mm/ -15%) (*Fig.8c, d*). Except for examining the range of △ET over certain year, the EM of multi-GCMs gives an averaged projection. The basin's mean △ET (if based on the ensemble mean of △T and △P in *Table2*) is likely going to increase 9 mm around 2025 and increase 23 mm around 2100. The △ET projection for the basin confidently points out that the whole basin's averaged △ET may increase in time. However, the regional △ET differ dramatically. Downstream region's averaged △ET increases 11 mm and upstream area raises 38 mm (in *Fig.8a*), which is similar to other scenarios that the averaged upstream △ET increases more than in the downstream region. Worth mentioning is that the differences between the upstream mean △ET and the downstream mean △ET are increasing dramatically in time, according to the comparison between (a) and (c) as well as (b) and (d) in *Fig.8*. Meanwhile these △ET differences of upstream-downstream also increase along with P decreasing, by comparing (a) with (b) or (c) with (d) in *Fig.8*.

Four spatial △PS distribution maps in *Fig.9* show the interaction between climate change and the water availability in the basin under same scenarios for examining the variations of △ET (refer to *Fig.8*). The whole basin's averaged △PS likely increases 6 mm and 7 mm (i.e. △PS= 6 mm and 7mm) in the near future (*Fig.9a*) and the distant future (*Fig.9c*) respectively under the wet scenario. In analogy, under the dry scenario the mean △PS may decrease 11 mm and 25 mm (i.e. △PS= - 11 mm and - 25mm) around 2025 and around 2100 (*Fig.9b,d*). Specifically, the averaged upstream ∆PS is likely to increase roughly 60 mm/year while for downstream ∆PS may decrease approximately 3mm/year, which gives an opposite direction in response to climate change. The conditions of ∆PS under the wet scenario in *Fig.9a,c* show that a large amount of water is available in the upstream region and the water there is able to generate surface water flows to downstream, feeding the delta and the Aral Sea.

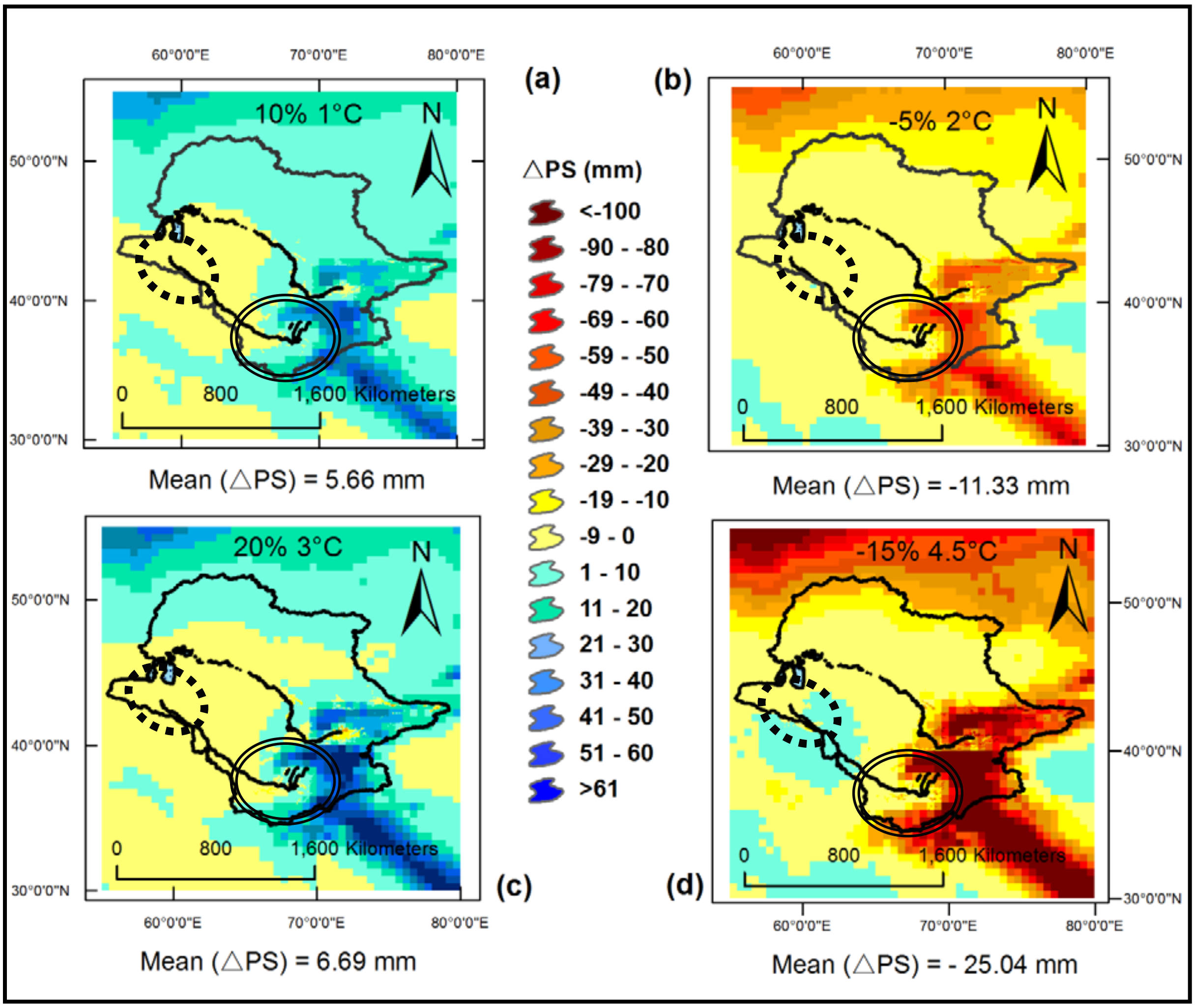

***Fig.9** The modeled ∆PS under two wet and two dry scenarios for near future (top two maps) and distant future (bottom two maps) predictions are showed in (a), (b); (c), (d) respectively. Two left maps are wet scenarios while two right maps stand for dry scenarios for the near future and the distant future projections correspondently. These four scenarios correspond to the wet or dry scenarios given in Fig.7 (with yellow points). Means of change within the whole ASDB (solid black line is the boundary of basin) are estimated and given below each map. The delta of Amu Darya is marked by dash black circle in each map while the upstream region is highlighted by solid double lines ellipse in each map.*

However, ∆PS conditions are changing dramatically under the dry scenario (in *Fig.9b,d*), especially the averaged water flux in upstream is going to decrease increasingly in time. For the near future, averaged ∆PS in upstream and downstream are all likely to decrease a certain amount. Nevertheless, the tipping condition might occur in the distant future around 2100 (*Fig.9d*). Namely, around 2100 the averaged downstream ∆PS is likely to increase 7 mm/year locally, instead of decreasing as basin's upstream where may experience an escalating decrease in water flux of 100mm/year loss (i.e. ∆PS= -100mm in upstream). Under this dry-distant scenario, the ∆PS between upstream and downstream has been changed considerably. Namely, the upstream region may have less water remained and available, which may not possible to supply surface runoff to downstream as it used to.

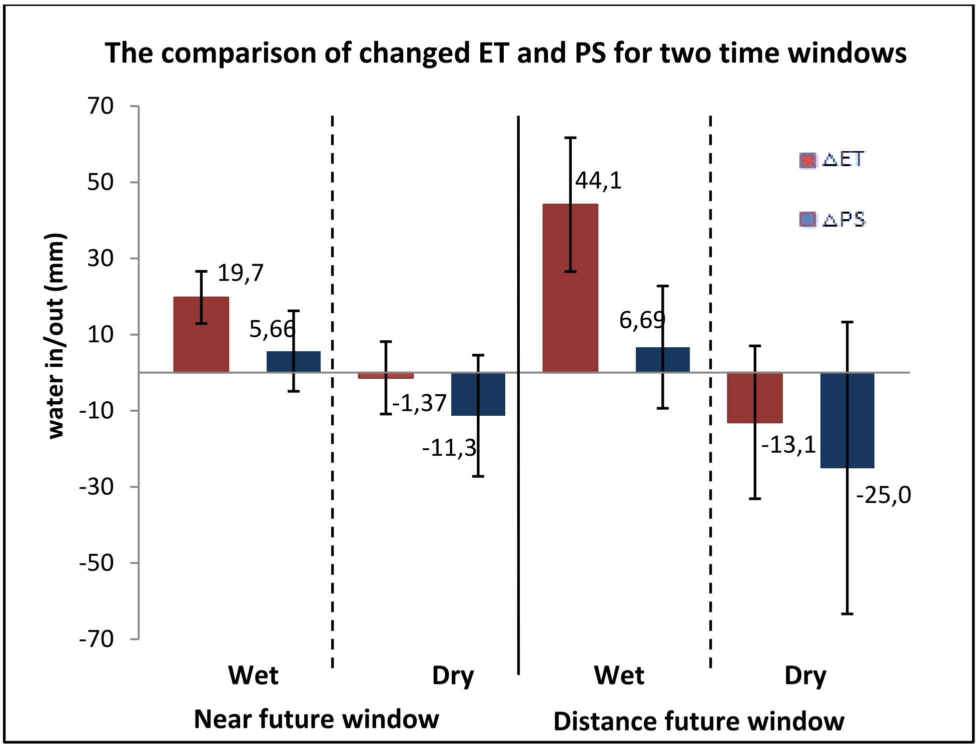

Fig.10 Comparison of the ensemble mean (colored bars) and standard deviation (error bars) for changed ET (in red) and PS (in blue) under four different considered wet or dry climate scenarios described in Fig. 8 and Fig. 9.

The linkage between ∆ET and ∆PS is addressed in *Fig.10*. The basin's ∆PS is to some extent accordant with the changing trend of ∆ET. Under the wet scenario, although the mean ∆ET in the near future is likely to increase much higher than in distant future, the corresponding increase of the ∆PS are almost the same amount in two time windows (*Fig.10*). Besides, around 2025, the distribution of both △ET and △PS stay in a small spread in space compared to the distant future predictions. Moreover, the △ET and △PS under wet condition might be less spatial heterogeneous across the basin (if comparing the standard deviations in *Fig.10*) than under dry condition. However, under dry scenarios, △ET and △PS both are going to decrease and their spatial variations are increasing dramatically in time (*Fig.10*).

4.3.2 River flow variations

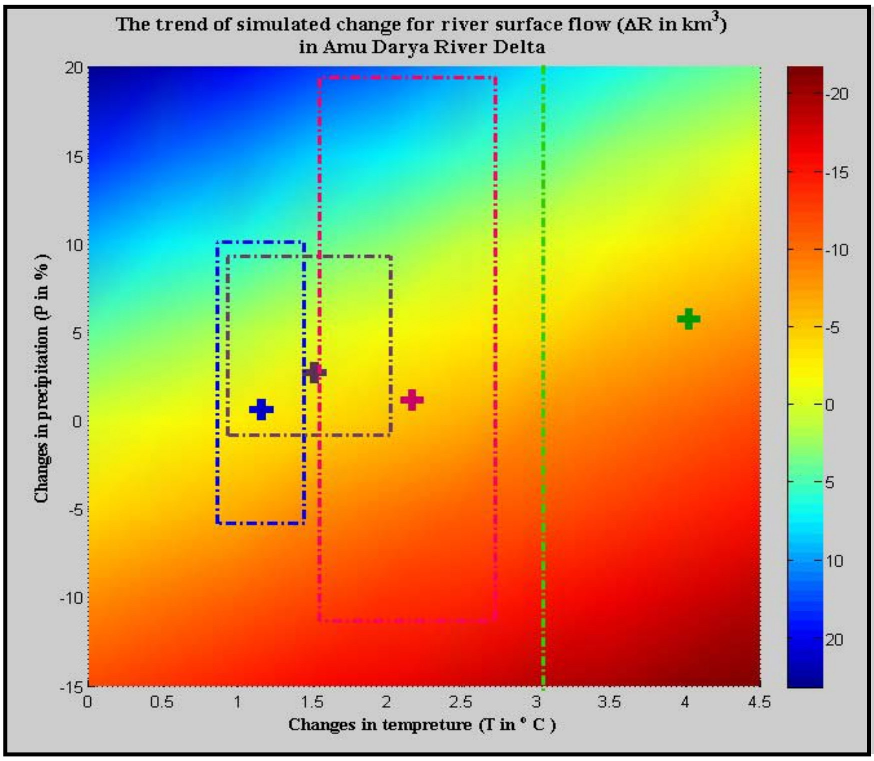

***Fig. 11** The general trend of estimated Hydrological Response Map for ΔR in the ADRD. On the surface of the Hydrological Response Map, four colored cross signals represent the mean values of four prediction envelopes correspond to Fig.7, P1, P2, P3, and P4 respectively. The colored dash rectangles stand for the prediction envelopes spanning over the surface of the Hydrological Response Map.*

Fig.11 shows a model-based Hydrological Response Map, which simulates a general trend of the surface river flow changes (△R) in the ADRD driven by the changing △T and △P. The changing △T and △P is the matrix of ($△T_i$, $△P_j$), where i=1,2,…, 10, j=1,2,…,8. (*Fig.11*). $△T_i$ is ranging from 0°C to 4.5°C with 0.5 interval and $△P_j$ is ranging from -15% to 20 % with 5 interval. The colored Hydrological

Response Map display values of ∆R in surface shape, ranging from - 20 km^3/year to 20 km^3/ year. Besides, *Fig.11* also combines the outputs from GCM projections by adding colored crosses to show the EM from each projection envelope and the colored dash rectangles to show the envelopes themselves (from *Fig.7* in **Section 4.2**). *Fig.11* shows that some single GCM's outputs yielding to a positive ∆R (i.e. an increase of ∆R), but over 83% of the outputs from single GCM are likely to tend to the decreasing direction. The EM of projections for all time windows congregates on yielding ∆R decrease. If only considering climate factors in near future by using EM from multi-GCM projections (i.e. blue and purple crosses in *Fig.11*), ∆R in delta is very possible to decrease approximately 3 km^3 every year. However, with the time prolonging, the predicted ∆R in the ADRD is very likely to decrease increasingly (*Fig.11*).

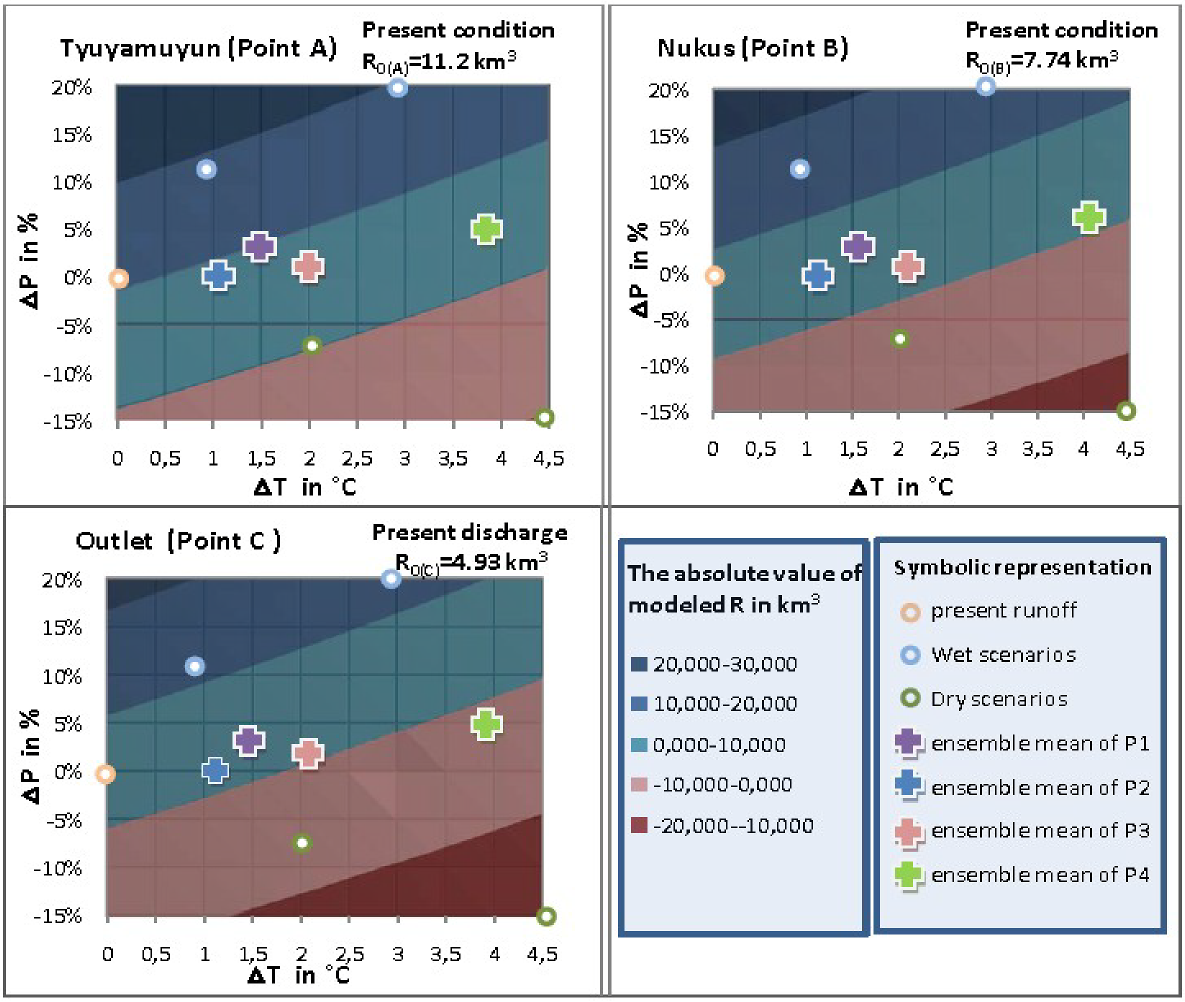

Fig. 12 Changes in the absolute R for three studied locations (Point A, B and C, which are specifically indicated in Fig.2).

Fig.12 summarizes the change of absolute R instead of △R by using Hydrological Response Map for three selected points (Point A, B and C) in the delta (*Fig.2*). Likewise, the EM values from multi-GCM projections and the considered wet and dry scenarios are displayed in each map (detailed values for three study sites referring to *Appendix1*). *Fig.12* shows the current river runoff in the upper delta segment ($R_{0(A)}$) (i.e. below Tyuyamuyun segment) is estimated 11.22 km^3/ year, mid reach segment (i.e. from Nukus), $R_{0(B)}$, is approximately 7.74 km^3/ year and discharge ($R_{0(C)}$) in Point C is 4.93 km^3/ year (*Fig.12)*. The lower reach near outlet has less surface water flow than in Tyuyamuyun and Nukus. By comparing the EM from the outputs of GCM projections for different time windows, although the change directions are all tend to the negative side (decreases of R) in each study site, in most of the cases water will still pass through the delta. However, until the scenarios for distant future (around 2100), the projection of the absolute R near outlet (in Point C) may experience a complete dry out and consequently the Aral Sea have no surface feeding at all (*Fig.12)*. If considering the wider range of projections' outputs, the hydrological conditions in future may change even worse.

4.4 Prediction of Tugai community's development based on their suitability

4.4.1 Suitability of Tugai

Here are synthesized hydro-climatic key factors that influence the Tugai in the ADRD, such as climate, water and soil conditions, are summarized in *Table3* with a suitability description, optimal range and references to original sources for all considered parameters. Specifically, T, P and ET can be considered as climate relevant parameters and *Table3* shows that the climatic toleration ranges for Tugai are incredibly wide. The water related suitability of Tugai is summarized by two main parameters: groundwater (GW) level and flooding regime. Regarding the GW level, a general optimal range of groundwater table (GWT, i.e. distance of groundwater table from soil surface) for Tugai community is ranging from 1 m to 5 m. However, different species' optimal living ranges are varying significantly and *Table3* provides the specific GWT demands for woody-bush Tugai, bush Tugai and grass decertified Tugai. Besides the level of GW, the quality of GW is studied and focused on groundwater salinity. GW

Table 3 Influential factors and correspondingly parameters, and the suitability, optimal range/ threshold and corresponding references to each parameters.

Factor	Parameter	Suitability description	Optimal Range	Reference
climate	**T**	Tolerate extreme temperatures	-40 ~ 40 °C	Rüger et al., 2003
	P	Tolerate very low precipitation	> 50 mm/year	Rüger et al., 2003
	ET	Tolerate very high evaporation	-	Rüger et al., 2003
water	**GW**	• GWT demands	1 ~5 m	Rüger et al., 2003
		- Woody-bush Tugai	1~1.5m	Novikova, 1998
		- Bush Tugai	2~4 m	Schlüter et al 2005
		- Grass decertified Tugai	3~5 m	Bakhiev&Treshkin, 1991
		• GW composition: salinity	0.5% ~2%	Rüger et al., 2005
			10 ~16 g/l	Novikova, 1998
		- Woody-bush Tugai on alluvium	non/slight salinity	Schlüter et al 2005
		- Bush Tugai:	salinity	Schlüter et al 2005
		- Grass decertified Tugai:	dry and salinity	Schlüter et al 2005
	flooding	could lower the salinity, links to GWT change	three years	Rüger et al., 2003
		- Frequency: in a row for Tugai establishment	at least 3 years	Novikova, 2001
		- Timing: in spring for adult woody-bush Tugai	up to 20 days	Schlüter et al 2005
		- Duration: neither short nor long less than	<2days/>30 days	Kuzmina&Treshkin,1997
soil	**salinity**	Thresholds for degradation/extinction	0.25% /0.45%	Kuzmina&Treshkin,1997
		Highest diversity found in non-saline soil	0.4%	Kuzmina&Treshkin,1997
		Optimal mean/median	1.3%/0.7%	Schlüter et al 2005
		Threshold for young Tugai	0.7%	Ma et al., 1997

salinity content generally can be tolerated between 0.5% and 2% and each species do have different tolerance levels. Furthermore, flooding regime is relevant to the suitability of Tugai, hence, frequency, timing and duration all influence Tugai's establishment and adult Tugai's development, which are explained in the detail by the optimal regime based on multiple studies (*Table3)*. Last, soil salinity determines Tugai's degradation, extinction and diversity and the salt composition percentage in *Table3* shows that the optimal mean is 1.3%. The threshold of the highest diversity is 0.4% while the threshold for young Tugai is 0.7%.

4.4.2 The responses of Tugai under changing hydro-climate

According to the suitability analysis (*Table3*), the projected climate for the study sites can be considered as suitable in the future. Even the temperature and precipitation in the wet and dry scenarios (*Fig.8,9*) will not excess the thresholds. Therefore, the climate factors cannot be expected to directly modify the future's Tugai distribution and diversity in the ADRD. Although *Fig.12* only presents that the magnitudes of annual mean runoff in three ADRD locations is likely to decease, such a decreased runoff will have small possibility to generate flooding regularly. Therefore, if the periodic flooding would not occur in the delta in three years (*Table3*), the Tugai productivity will decrease significantly. On the other hand, the runoff decease (*Fig.11*) in the future will highly limit the capacity of feeding ground water, which may lower the GWT to some extent. In *Fig.11* for wet scenarios (both for near future and distant future), the annual discharge may increase significantly which could increase Tugai establishment especially for woody-bush Tugai (*Table3*). In the contrary, the dry scenarios would give negative effect on Tugai in the future in terms of degradation and extinction. Besides, the increment of salinity partially is caused by high ET (*Fig.8*), the absence of flooding and low river flow (*Fig.11*). Specifically, the wet scenarios (ET increases (*Fig.8a,c)* but PS increases (*Fig.9a,c)* and river R increases (*Fig.11*,*12*)) have large probabilities to decrease salinity than the dry scenarios, however, the salinity under the dry scenarios may increase due to local ET is going to decrease.

Less water in the region may urge the surrounding desert expanding. Hence, once the desertification and salinization occurred severely, the transition between the Tugai communities become actively. For instance, the slightly less salt tolerant woody-bush species (i.e. poplar or willow) along the river may largely decrease from the delta, and the bush Tugai (e.g. salt cedar and liquorice) is likely to replace by more dry resistant and salt tolerant species like *Halostachys caspica* (*Table3*). Besides, the similar change would take place in grass Tugai, which reverse to more desert species like the Camel thron (*Alhagi pseudalhagi*). The transition of Tugai formation will further lead to lower the species diversity and decrease the fragmentation of remaining Tugai.

5. Discussion

5.1 Hydro-climate dynamics in the Amu Darya River Basin

The downstream-upstream relationship of water flux in the ADRB was studied by other researchers (e.g. refer to Jarsjö et al., 2011; Shibuo, et al., 2007; Novikova, 2001; Micklin, 2004, Gordon et al. 2008; Lobell et al., 2009) and they found that river runoff in the ADRB is almost exclusively from glacier and snowmelt in the high mountainous areas of Tajikistan, Afghanistan and Kyrgyzstan. Although today's climate with a rather high ET in upstream region relevant to average ET in basin, still the local comparatively low T and high P is likely to create large water potential for whole basin. However, owing to large water withdraw for irrigation in upstream regions the downstream delta has suffered from an inadequacy of water as inflow (Micklin, 2004). Additionally, the climate in the downstream delta, high T, low P and high ET makes it hard to sustain and conserve water locally (e.g. in river reservoirs, canals, groundwater reservoirs, etc.). Even the surface water is insufficient to feed the groundwater in downstream. Regional climate and its irrigation scheme has further elevated the delta's salinity caused by repeated water usage in the middle and upper reaches of the Amu Darya River (Glantz, 2005). Furthermore, the relationship of surface water flux between upstream and downstream pushes to consider water flux in a relatively small region, such as the downstream delta region. The upper and middle reach of the delta areas are covered by intensely irrigated fields, but because of the changing land and water condition, the irrigated fields becomes less productive and satisfactory. Changes in the water flux dynamics in terms of general discharge, river delta, and river month have important implications for water resource management in the future.

One result from this study shows that local ET in middle and upper reaches is higher than the mean level of the basin, while the lower reach delta near the outlet of Aral Sea has lower ET. As other studies also found that the large-scale irrigated lands may enlarge the potential for water loss from the irrigation canal or fields (Jarsjö et al., 2011; Shibuo, et al., 2007). Consequently, the irrigation driven high ET largely alters the water flux in the whole basin and strongly influences the local climate. As studies stated that in the whole ASDB, water losses in agricultural sector are mainly originated from old and inefficient irrigation channel networks, inefficient irrigation practices, and failure water saving techniques (Froebrich and Kayumov, 2004; Törnqvist and Jarsjö, 2011). This fact shows that the irrigation scheme increases water loss, which should be appropriately regulated during the development decision-making process. Effective human intervention for downstream of the ASDB to a large extent can change exiting hydro-climatic status, such as by introducing water saving techniques, implementing sustainable agriculture practices, reconstructing water distribution system or pioneering drought-resistant high-yield crops. These measures may increase the resilience of natural resources and mitigate the hydro-climate induced changes.

Changes in the temporal and spatial variability of hydro-climatic parameters are also important to reflect both water and human vulnerability in different locations of the ADRB. Cities located in the delta have suffered severe water shortage for decades under different pressures and this situation is increasingly worse with population expansion (Micklin, 2004; Cai, et al., 2003). Besides, water exports through the Karakum canal and other irrigation canals crossing the ADRB boundary annually volume is 4 times larger than the current discharge at the mouth (Jarsjö et al., 2011). Anthropogenic impacts to water resources system have resulted in changes of the interactions between climate and hydrological cycle. Especially arid areas all over the world are highly susceptible to the human interventions, thus any human activities on the landscape will change the hydro-climate condition in return sensitively (Glantz, 2005). Therefore, a detailed local hydro-climatic projection for the local management is a solid reference than large scale climate change information.

5.2 Uncertainty of GCMs driven projections on hydro-climatic condition

The Hydrological Response Map in this study is using ΔT ranges from 0°C to 4.5°C with 0.5 interval and ΔP from -15% to 20 % with 5 interval to simulated the effects of climate change on river flow for the ADRB. Relevant studies have simulated the response of climate change partially to global hydrological system and partly to a rather large region (refer to Arora and Boer, 2001), a widely-accepted range of the hypothetical scenarios, the air temperature rises by 1 ~ 4°C and the precipitation changes (rise or fall) 0 ~ 10%, which is similar to the range has been used in this study. Therefore, the climate change projections considered for the ASDB is relatively consistent to the global climate change trend.

The hydro-meteorological changes in the ASDB are projected to experience significant changes in the future under a series of global warming scenarios, and projected changes in T, P, ET, PS and R showed the considerable variability and uncertainties between different GCMs-driven climatic projections in time and space. But trend of ensemble mean for the considered time periods (near future, mid-century and distant future) is consistent. However, the credibility of the results depends on many aspects. The climate-induced hydrological projections normally associated a series of the uncertainties with: (1) the uncertain climate projections generate the unreliable inputs to the hydrological model; (2) the process of coupling GCM scenarios with hydrological models has involved marvelous simplification and assumptions caused by the coarse resolution (a horizontal resolution of between 250km and 600km, 10 ~ 30 vertical layers in the atmosphere) and the insufficiency of spatial scale on existing models and downscaling techniques for regional or local context (especially in the zones with complex topography such as the ASDB (Liubimtseva et al. 2009)); (3) the complexities of temperature and precipitation changes and non-linear climatic responses on hydrological cycle. As other studies (e.g. Jarsjö et al., 2011) mentioned that the corresponding EM values from multi-GCMs is normally more consistent with the historical observation values. Hence, this study uses multi-GCMs’ ensemble mean instead of using single GCMs performance to investigate the climate change impact on hydrological responses in a rather large basin scale. The surface of the basin covers a reasonable number of GCM grid cells, which diminishes the first two inherent uncertainties caused by the modeled-related biases in hydro-climatic change projections (refer to study down by Jarsjö et al. (2011) and Rajagopalan et al. (2002)). Besides, the variability and sensitively of natural system itself poses great challenges to draw a clear trend of future changes. Although the multiple uncertainties hinder to fully understand the system, the implications of study results offer a great basis to examine the uncertainty by considering the wet and dry scenario for different time scales and also provide possibility to gain more robust projections for regional river flow and locally created water flux.

Information on the changes of R resulting by climatic driving variables could provide insights to environmental impacts assessment not only for the single river catchment in regional scale but also for the specific locations of river delta in a rather small local scale. Climate change might also affect snow and ice storage, the increased T in the Pamir Mountains may increase the potential of water availability in upstream of ADRB. However, future irrigation scheme plan announced by Central Asia countries still doesn't give an optimistic signal: the irrigation expansion may increase and hydropower in upstream might increase and strongly regulated (Jarsjö et al., 2011). Hence, increasing melting water would be able to balance the water withdraw along the river cause by irrigation and river runoff is very unlikely to increase (Liubimtseva et al. 2009). From results of this study give a general message that the surface water availability in downstream is likely to decrease till year around 2100 river flow may disappear totally in the delta.

5.3 Ecosystem management in the Amu Darya River Delta

The dynamics between hydro-climate and Tugai for the ADRD quantified in this study provides important basis for the formulation of more robust forecasts on the future environmental development in the ADRD and further for recommendation of measures for mitigation of environmental deterioration. However, the response of Tugai to hydro-climatic change is complex which is hard to draw a conclusion on which factor determines the condition of riparian vegetation change in the delta. Except for the hydro-climatic influential factors, the anthropogenic impacts also determine the transformation of Tugai and decline of Tugai's biodiversity. Overexploitation is one of critical pressure to the condition of Tugai (Kuzmina and Treshkin, 1997). Namely, overgrazing in the delta gives rise to the destruction of Tugai species, the degradation of the upper soil layers and the desertification (Novikova et al., 1998; Treshkin et al., 1998). Therefore, the preservation of Tugai is an urgent and initial measure to protect the remaining forest patches, especially overgrazing as one of the strictest human activities on the ecosystem must be controlled (Novikova et al., 1998). Second, restoration is required in suitable sites. Besides, Rüger et al. (2005) stated that under the present low GWT condition more frequent flooding is necessary to prevent Tugai. Hence, producing an artificial flood is an effective measure to facilitate young Tugai to enable reestablishment. Additionally, afforestation and the setup of tree nurseries are suggested to be able to establish resilience ecosystem in the delta (Novikova et al., 1998; Treshkin et al., 1998).

6. Conclusion summary

- The EM of outputs from 65 GCMs' projections gives a possible trend of the regional △T in the ASDB is likely to continuously increase 1.5 °C ~ 4°C in time till 2100, while, the regional △P may increase 5 mm/year to 13 mm/year in time from near future to distant future with a large variation and uncertainty. Although some single GCM's outputs yielding to an increase of △R, over 80% of the outputs from single GCM projections and EM of the multi-GCM projections are likely to congregate on yielding △R decrease. With the time prolonging, the predicted △R in the ADRD is very likely to increasingly decrease, ranging from decreasing 3 km^3/ year around 2025 to decreasing 7 km^3/ year around 2050. Till 2100, the projected absolute R may experience completely no surface flow and dry out near outlet.
- The △ET projection for the whole basin confidently points out that the averaged △ET may increase in time. The basin's △PS is to some extent accordant with the changing trend of △ET. However, the regional △ET and △PS differ dramatically in upstream and downstream. Under wet scenarios, a large amount of water is available in upstream region and the water there is able to generate surface water flows to downstream, feeding the delta and the Aral Sea. Under dry scenario, the tipping point might occur around 2100 and the △PS in upstream and downstream has been changed considerably. Therefore, water in upstream region will have less water remained and available, which may not possible to supply surface runoff to downstream as it used to.
- Due to high likelihood of decreased R in the delta, the desertification and salinization may occur severely, hence, the tran1sition between the Tugai communities will become actively. The slightly less salt tolerant woody-bush species along the river may largely decrease from the delta, and the bush Tugai is likely to replace by more dry resistant and salt tolerant species. Furthermore, the similar change would take place in grass Tugai, which reverse to more desert species. The transition of Tugai formation will further lead to lower the species diversity and decrease the fragmentation of remaining Tugai. Consequently, the preservation of Tugai is an

urgent and initial measure to protect the remaining forest patches, followed by restoration Tugai through artificial flooding combined with afforestation.

Acknowledgements

To be a student in Stockholm University is an excellent education experience to me. I gained different knowledge and expanded my social networks. I believe that not only the fascinating courses time, but also the time I spent on doing thesis project was all indelible and beneficial to my life and future career. I would like to thank all who supported me during my thesis work. One person deserves my big thanks and sincerest gratitude is my supervisor, Dr. Jarsjö Jerker, who supported me throughout my thesis with tremendous patience and abundant knowledge, who gave me encouragement and effort, who cultivate me my academic competence. Moreover, as a co-supervisor, Rebecka Törnqvist, she helped me to figure out some technique problems patiently and I would like to show my gratitude and wish you newborn boy happy and healthy. Besides, I also want to thank Dr. Steve Lyon who agreed to be my examiner and allowed me to follow my own working rhythm. For sure, thank all teachers and fellow students who gave me inspirations during my study and who shared knowledge with me. Of course, I want to express my deep thank to my parents, without whose understanding and support I could never become to a person who I am now. I love you two. Finally, I especially wish to thank my fiancé, Ning, for his eternal love, patience and understanding. With all my love, I want to say 'THANKS' to all.

References

Asarin, A.E., Kravtsova, V. I. and Mikhailov, V. N. (2009). Amudarya and Syrdarya Rivers and Their Deltas. *Hdb Envi Chem*., 7:101-121, DOI 10.1007/698_2009_8.

Arora, V. K. and Boer, J.G. (2001). Effects of simulated climate change on the hydrology of major river basins. *Journal of geophysical research*, 106 (4): 3335-3348.

Arnell, N.W. (2003). Effects of IPCC SRES emissions scenarios on river runoff: a global perspective. *Hydrology and Earth System Sciences*, 7 (5): 619-641.

Bakhiev AB, Treshkin SE. (1991). Dynamics of the productivity of Tugai communities in the delta of the Amudarya under the influence of a changing hydrological regime of the territory. *Journal of the Karakalpak Branch of the Uzbek Academy of Sciences*: 19-22.

Cai, Ximing, McKinney, D. C. and Rosegrant, M. W. (2003). Sustainability analysis for irrigation water management in the Aral Sea region. *Agricultural Systems,* 76(3): 1043-1066.

Chub, V.E. (2007). Water resources of the Central Asia under conditions of climate change. *Climate change and terrestrial carbon sequestration in central Asia.* [Lal R, Suleimenov M, Stewart BA, Hansen DO, Doraiswamy P (eds)], CRC Press, Taylor & Francis: 494.

Crosa, G., Froebrich, J., Nikolayenko, V., Stefani, F., Galli, P., Calamari, D. (2006). Spatial and seasonal variations in the water quality of the Amu Darya River (Central Asia). *Water Res.* 40, 2237-2245.

De Wit, M., Meinardi, C., Wendland, F. and Kunkel, R. (2000). Modelling water fluxes for the analysis of diffuse pollution at the river basin scale. *Hydrological Processes,* 14:1707–1723. DOI:10.1002/1099-1085(200007)14:10<1707::AID-HYP64>3.0.CO;2-E.

Froebrich, J. and Kayumov, Odil. (2004). Water management aspects of Amu Darya-options for future strategies. [J.C.J.Nihoul et al. (eds.)], *Dying and Dead Seas,* Ch 2: 49-76.

Farr, T. G., Rosen, P. A., Caro, E., Crippen, R., Duren, R., Hensley, S., Kobrick, M., Paller, M., Rodriguez, E., Roth, L., Seal, D., Shaffer, S., Shimada, J., Umland, J., Werner, M., Oskin, M., Burbank, D., and Alsdorf, D. E. (2007). The shuttle radar topography mission*, Rev. Geophys.,*45, RG2004, DOI:10.1029/2005RG000183.

Gordon, L. J., Peterson, G. D., and Bennett, E. M. (2008).Agricultural modifications of hydrological flows create ecological surprises. *Trends Ecol. E.* 23: 211–219.

Glantz, M.H. (2005). Water, climate, and development issues in the Amu Darya basin. *Mitigation and Adaptation Strategies for Global Change,* 10 (1): 23–50.

Glantz, M.H. (2009). Foreword for Environmental Problems of Central Asia and their Economic, Social and Security Impacts. *Environmental Problems of Central Asia and their Economic, Social and security Impacts*, Springer science and Business Media B.V.:99-107.

Global Runoff Data Centre (GRDC) in Koblenz, Germany, available at http://grdc.bafg.de.

IPCC (2003). Solomon, S., Qin, D., Manning, M., Chen, Z., Marquis, M., Averyt, K.B., Tignor, M., Miller, H.L. (Eds.), Climate Change 2003: the Physical Science Basis. Contribution of Working Group I to the Third Assessment Report of the Intergovernmental Panel on Climate Change. Reviewed at: 2011.5.10 [http://www.ipcc.ch/publications_and_data/]

IPCC (2007a). Solomon, S., Qin, D., Manning, M., Chen, Z., Marquis, M., Averyt, K.B., Tignor, M., Miller, H.L. (Eds.), Climate Change 2007: the Physical Science Basis. Contribution of Working Group I to the Fourth Assessment Report of the Intergovernmental Panel on Climate Change. *Cambridge University Press, Cambridge, United Kingdom and New York,* NY, USA, 996.

IPCC (2007b). Parry, M.L., Canziani, O.F., Palutikof, J.P., van der Linden, P.J., Hanson, C.E. (Eds.), Climate Change 2007: Impacts, Adaptation and Vulnerability. Contribution of Working Group II to the Fourth Assessment Report of the Intergovernmental Panel on Climate Change. *Cambridge University Press, Cambridge, UK, and New York,* NY, USA, 976.

Johansson, O., Aimbetov, I. and Jarsjö, J. (2009). Variation of groundwater salinity in the partially irrigated Amudarya River delta, Uzbekistan. *Journal of Marine Systems*,76(3): 287-295.

Jarsjö, J., Asokan, Shilpa M., Shibuo, Y., and Destouni, G. (2008). Water scarcity in the Aral Sea Drainage Basin: Contributions of Agricultural Irrigation and Changing Climate. *Environmental Problems of Central Asia and their Economic, Social and security Impacts*, Springer science and Business Media B.V.:99-107.

Jarsjö, J, Asokan, Shilpa M., Prieto, C., Bring, A., and Destouni, G. (2011). Hydrological responses to climate change conditioned by historic alterations of land-use and water-use. *Hydrology and Earth System Science Discussions,* 8: 7595–7620. DOI:10.5194/hessd-8-7595-2011.

Jarsjö, J and Tornqvist R. (2010a). Groundwater quality, climate and irrigation: Large-scale, long-term trends in the Aral Sea Drainage Basin. *Groundwater quality management in a rapidly changing world* (Proc.7th International groundwater quality conference held in Zurich, Switzerland):13-18.

Jarsjö, J and Tornqvist R. (2010b). Transport of water-borne contaminants under climate change and land-use change in Central Asia. *Journal of Contaminant Hydrology (in review).*

Kulmatov R. (2009). Modern problems in using, protecting and managing water and land resources of the Aral Sea Basin. *Environmental Problems of Central Asia and their Economic, Social and security Impacts.* Springer science and Business Media B. 1:15-29.

Kuzmina, Z. and Treshkin, S. (1997). Soil salinization and dynamics of Tugai vegetation in the Southeastern Caspian Sea Region and in the Aral Sea Coastal Region. *Eurasian Soil Science 30*(6), 642–649.

Langbein, W. B. (1949). Annual runoff in the United States, US Geological Survey Circular: Simulated impacts of irrigation on the atmospheric circulation over Asia. *J. Geophys. Res.-Atmos.*, (116), D08114, 30. doi:10.1029/2010JD014740, 2011.

Lioubimtseva, E., Cole, R., Adams, J.M. and Kapustin, G. (2005). Impacts of climate and land-cover changes in arid lands of Central Asia. *Journal of Arid Environments*, 62 (2): 285–308.

Lioubimtseva, E. and Cole, R. (2006). Uncertainties of Climate Change in Arid Environments of Central Asia. *Reviews in Fisheries Science,* 14: 29–49. DOI: 10.1080/10641260500340603.

Lioubimtseva, E. and Henebry, G..M. (2009). Climate and environmental change in arid Central Asia: Impacts, vulnerability, and adaptations. *Journal of Arid Environments,* 73(I, 11): 963-977.

Lobell, D., Bala, G., Mirin, A., Phillips, T., Maxwell, R., and Rotman D. (2009). Regional differences in the influence of irrigation on climate. *J. Climate*, 22, 2248–2255.

Ma, H.C., Fung, L., Wang, S.S., Altman, A. and Hüttermann, A. (1997). Photosynthetic response of *Populus euphratica* to salt stress. *Forest Ecology and Management, 93*: 55–61.

MacDonald, G. J. and Sertorio L. (1990). Global climate and ecosystem change. *NATO ASI Series,* 240 (1,97): 141,157.

Mamatov, S. (2003). Study of the Groundwater Contribution to the Aral Sea Region Water Supply and Water Quality: *Strategies for Reversibility and Pollution Control-INTAS project 1014.* EU-INTAS Aral Sea Basin Call 2000, Group CR5status report.

Micklin,P. (2002). Water in the Aral Sea basin of Central Asia: cause of conflict or cooperation. *Eurasian Geography and Economics.* 43(7): 505-528.

Micklin, P. (2004). The Aral Sea Crisis. *Environmental Problems of Central Asia and their Economic, Social and security Impacts.* Springer science and Business Media B.:99-118.

Mitchell, T. D., and Jones. P. D. (2005). An improved method of constructing a database of monthly climate observations and associated highresolution grids,. *Int. J. Climatol*., 25:693–712.

Milly, P. C. D., Dunne, K. A., and Vecchia, A. V. (2005). Global pattern of trends in streamflow and water availability in a changing climate. *Nature*, 438: 347–350.

Nakagawa, T. et al. (2003). Asynchronous climate changes in the north Atlantic and Japan during the last termination. *Science*, 299, 688 691, DOI:10.1126/science.1078235.

Nijssen, B., O'Donnell,G.M., Hamlet, A.F. and Lettenmaier, D. P. (2001). Sensitivity of Global Rivers to Climate Change. Climatic Change , 50: 143–175.

Novikova NM, Kust GS, Kouzmina JV, Trofimova GU, Dikariova, TV, Avetian SA, Rozov SU, Deruzhinskaya VD, Safonicheva LF, Lubeznov UE. (1998). Contemporary plant and soil cover changes in the Amudarya and Syrdarya river deltas. In: UNESCO (ed), Ecological Research and Monitoring of the Aral Sea Deltas, Book 1. UNESCO, Paris.

Novikova, N., J. Kuzmina, Dikareva, T. andTrofimova, T. (2001). Preservation of the Tugai biocomplex diversity within the Amu–Dar'ya and Syr–Dar'ya river deltas in aridization conditions.*Ecological Research and Monitoring of the Aral Sea Deltas – A basis for restoration*, 2. UNESCO Aral Sea Project.

Qi, Jiagou and Kulmatov, R. (2008). An overview of Environmental Issues in Central Asia. Environmental Problems of Central Asia and their Economic, Social and security Impacts. Springer science and Business Media B.V.:3-11

Rajagopalan, B., Lall, U. and Zebiak, S. E. (2002). Categorical climate forecasts through regularization and optimal combination of multiple GCM ensembles. *Mon. Weather Rev.,* 130: 1792–1811.

Rüger, N., Schlüter M. and Matthies, M. (2003). A fuzzy habitat suitability index for Populus euphratica in the Northern Amudarya delta (Uzbekistan). *Ecological Modeling,* 184 (2-4): 313-328, DOI:10.1016/j.ecolmodel

Savitsky, A.G., Schlüter, M., Taryannikova, R.V., Agaltseva, N.A., Chub, V.E. (2007). Current and future impacts of climate change on river runoff in the Central Asian river basins. *Adaptive and integrated water management—coping with complexity and uncertainty*. Springer. Pahl-Wostl C, Kabat P,Moeltgen J (eds) .

Schlüter, M. Khasankhanova, G., Abdullaev, U., Talskikh, V., Taryannikova, R., Joldasova, I. (2003). Incorporating environmental flows into water management in the Amudarya river delta. Reviewed[http://www.newater.info/caiwa/data/papers%20session/H2/Schlueter_et_al_final.pdf] at 2011.10.24.

Schlüter, M., Savitsky, A.G., McKinney, D.C. and Lieth, H. (2005). Optimizing long-term water allocation in the Amudarya River delta: a water management model for ecological impact assessment. *Environmental Modeling & Software*, 20: 529-545, DOI:10.1016/j.envsoft.2004.03.005.

Schlüter, M. and Rüger, N. (2007). Application of a GIS-based simulation tool to illustrate implications of uncertainties for water management in the Amudarya river delta. *Environmental modeling and software*. 22: 158-166.

Shibuo, Y., Jarsjö, J. and Destouni, G. (2007). Hydrological responses to climate change and irrigation in the Aral Sea drainage basin, *Geophys. Res. Lett.,* 34, L21406, DOI:10.1029/2007GL031465.

Stakhiv, E., Lins, H. andShiklomanov, I. (1992). Hydrology and water resources. *The Supplementary Report to the IPCC Impacts Assessments* [McG. Tegart, W.J. and G.W. Sheldon (eds.)]. Australian Govt. Publ. Service, Canberra, Australia, 71-83.

Siebert, S., Döll, P., Feick, S. and Hoogeveen, J. (2005). Global map of irrigated areas version 3, *Inst. of Phys. Geogr.,* Univ. of Frankfurt, Frankfurt, Germany.

Thomas, F.S., Arndt, S., Bruelheide, H., Foetzki, A, Gries, D., Huang, J., Popp, M., Wang, G., Zhang, X., Runge, M. (2000). Ecological basis for a sustainable management of the indigenous vegetation in a Central-Asian desert: Presentation and first results. *Journal of Applied Botany*, 74: 212-219.

Treshkin, S. Y., Kamalov, S., Bachiev, A., Mamutov, N., Gladishev, A. and Aimbetov, I. (1998). Present status of the Tugai forests in the lower Amu–Dar'ya Basin and problems of their protection and restoration. *Ecological Research and Monitoring of the Aral Sea Deltas –A basis for restoration*. UNESCO Aral Sea Project.

Treshkin, S. (2001).The Tugai forests of floodplain of the Amudarya river: Ecology, dynamics and their conservation. *Sustainable Land Use in Deserts*, [S.W. Breckle, M. Veste, and W. Wucherer (Eds.)], Springer, 95–103.

Törnqvist, R. and Jarsjö, J. (2011). Water savings through improved irrigation techniques: Basin-scale quantification in semi-arid environments. *Water Resource Management, Online First™,* DOI:10.1007/s11269-011-9819-9

Törnqvist, R., Jarsjö, J., Karimov , B. (2011). Health risks from large-scale water pollution: Trends in Central Asia*. Environment International*, *37 (2)*: *435-442*

Turc, L. (1954). The water balance of soils: Relation between precipitation evaporation and flow. *Ann. Agron.,* 5, 491– 569.

Van, D. R. (1999). Coastal vulnerability assessment: assessing vulnerability to climate change and sea level rise. *ERISS Internal Report 313*: ch1, Jabiru, Australia.

Zonn, I., Glantz, M., Kostianoy, A., Kosarev,A. (2009). The Aral Sea Encyclopedia. Springer, DOI: 10.1007/978-3-540-85088-5

Appendix

Appendix 1 ***The modeled absolute values of annual river runoff in Tyuyamuyun, Nukus, and outlet under four different scenarios compared to the current river runoff (baseline) in each studied location.***